

This is an Open Access document downloaded from ORCA, Cardiff University's institutional repository: <https://orca.cardiff.ac.uk/id/eprint/97371/>

This is the author's version of a work that was submitted to / accepted for publication.

Citation for final published version:

Bonifazi, Davide 2017. Versatile self-adapting boronic acids for H-bond recognition: from discrete to polymeric supramolecules. *Journal of the American Chemical Society* 139 (7) , pp. 2710-2727. 10.1021/jacs.6b11362

Publishers page: <http://dx.doi.org/10.1021/jacs.6b11362>

Please note:

Changes made as a result of publishing processes such as copy-editing, formatting and page numbers may not be reflected in this version. For the definitive version of this publication, please refer to the published source. You are advised to consult the publisher's version if you wish to cite this paper.

This version is being made available in accordance with publisher policies. See <http://orca.cf.ac.uk/policies.html> for usage policies. Copyright and moral rights for publications made available in ORCA are retained by the copyright holders.



Versatile self-adapting boronic acids for H-bond recognition: from discrete to polymeric supramolecules

Irene Georgiou,[†] Simon Kervyn,[†] Alexandre Rossignon,^{†,§} Federica De Leo,[†] Johan Wouters,[†] Gilles Bruylants,[‡] and Davide Bonifazi^{*,†,§}

[†]Department of Chemistry, University of Namur (UNamur), Rue de Bruxelles 61, 5000, Namur, Belgium; [‡] Université Libre de Bruxelles, Ecole Polytechnique de Bruxelles, Campus du Solbosch, Avenue F. D. Roosevelt 50, 1050, Bruxelles, Belgium; [§]School of Chemistry, Cardiff University, Park Place, Main Building, CF10 3AT, Cardiff, UK.

ABSTRACT: By taking advantage of the peculiar dynamic covalent reactivity of boronic acids to form tetraboronate derivatives, interest has risen to use the aryl derivatives in materials science and supramolecular chemistry, nevertheless their ability to form H-bonded complexes has been only marginally touched. Herein we report the first solution and solid-state binding studies of first double H-bonded DD•AA-type complexes of a series of aromatic boronic acids that adopt a synsyn conformation with suitable complementary H-bonding acceptor partners. The first determination of the K_a in solution of ortho substituted boronic acids showed that 1:1 association is in the range between 300 and 6900 M⁻¹. Crystallization of dimeric 1:1, trimeric 1:2 and 2:1 complexes enabled in depth examination of these complexes in the solid state, proving the selection of the -B(OH)₂ syn-syn conformer through a pair of frontal H-bonds with the relevant AA partner. Non-ortho substituted boronic acids result in “flat” complexes. On the other hand, sterically demanding analogues bearing ortho-substituents strive to retain their recognition properties rotating the ArB(OH)₂ moiety forming “T-shaped” complexes. Solid-state studies of a diboronic acid and a tetraazanaphthacene provided for the first time the formation of a supramolecular H-bonded polymeric ribbon. Given the conformational dynamicity of the -B(OH)₂ functional group, it is expected that these findings will also open new possibilities in metal-free catalysis or organic crystal engineering, where double H-bonding donor boronic acids could act as suitable organocatalysts or templates developing functional materials with tailored organizational properties.

INTRODUCTION

Organoboronic acids are an important group of compounds that has risen to its highest impact since their use in organic synthesis and medicinal chemistry.¹ However, great interest has been also recently reserved for applications in supramolecular chemistry,² sensing³ and organic catalysis⁴ by taking advantage of the peculiar dynamic covalent reactivity⁵ of ArB(OH)₂ and its dehydrated derivatives, to engineer a large variety of architectures resulting from boronate esterification,⁶ boroxine⁷ and spiroborate formation,⁸ to name a few.

However, the ability to form H-bonded complexes and their exploitation in molecular recognition has been relatively unexplored.² H-bonded architectures are often obtained exploiting the self-association of organoboronic acids that form polymeric 2D and 3D H-bonded architectures at the solid state,⁹ with phenylboronic acid being one of the first examples reported.^{9,10} In these systems, homodimers are formed and then organized as tapes, in which the ArB(OH)₂ functionalities adopt a *syn-anti* conformation (Figure 1a) triggering the formation of frontal DA•AD complexes, which are held together by lateral intermolecular H-bonds.¹⁰ Diamondoid-like 3D architectures could also be obtained when a tetratopic building block, tetrahedrally exposing four arylboronic acids, is used.¹¹ When a 2-methoxy substituted ArB(OH)₂ is employed, the boronic acid moiety is locked into the *syn-anti* conformation through an intramolecular H-bond involving one hydroxyl group and the oxygen heteroatom situated in the *ortho* position.¹² At the solid state, this restricts the formation of the architectures only to dimers. A similar behavior is observed for *ortho*-substituted ArB(OH)₂ bearing an imino, aminomethyl or azo groups.¹³ Weak intramolecular H-bonds are also observed in the presence of fluorine atoms.¹⁴ On the other hand, when a 2,6-dimethoxy substituted ArB(OH)₂ is used, the hydroxyl groups adopt an *anti-anti* conformation (Figure 1c), disfavoring the formation of intermolecular H-bonds, thus leading to monomeric species at the solid state.¹⁵ *Anti-anti*

conformation can be also observed at the solid state in co-crystals containing either urea derivatives^{16a} or carboxy groups^{16b}. Finally, *syn-syn* ArB(OH)₂ are seldom observed in DD•AA type complexes, the latter being essentially restricted to co-crystals containing carboxylates,^{17a-c} bis-pyridine,^{17d-g} or 1,10-phenanthroline^{17h} (Figure 1b). In a very recent work it has been postulated that the *syn-syn* conformer of a variety of ArB(OH)₂ is the active catalytic specie in the fixation of CO₂ with epoxides to give the corresponding cyclic carbonates with excellent yields.¹⁸

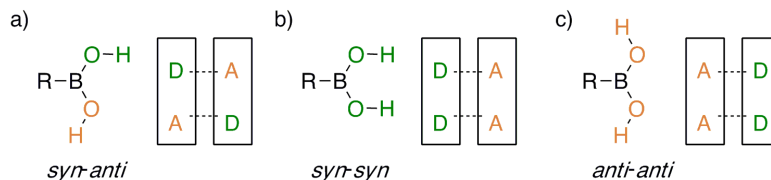
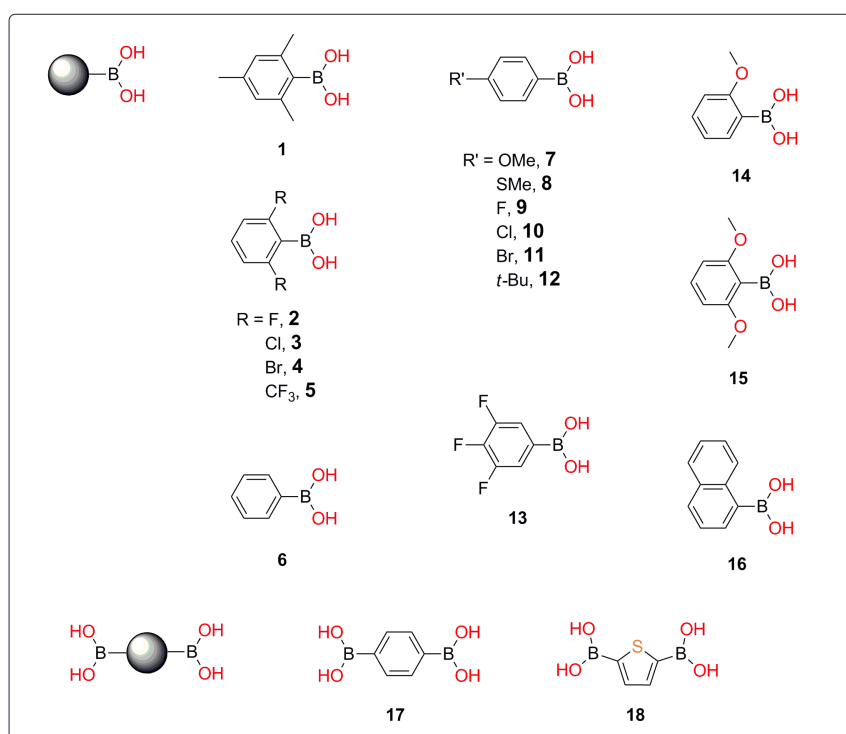
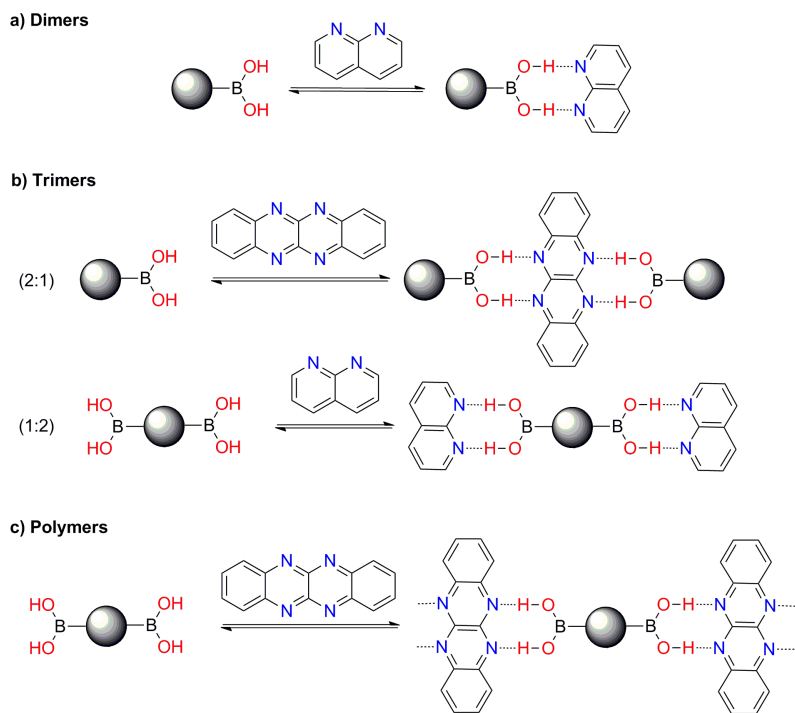


Figure 1. Structural representation of the (a) *syn-anti*, (b) *syn-syn* and (c) *anti-anti* conformation of the boronic acid RB(OH)₂ functionality, adopted when acting as a DA, DD and AA system respectively in DA•AD, DD•AA and AA•DD complexes. D and A are the H-bonding functional group donors and acceptors, respectively.⁸⁻¹⁷

Although the evidence for the formation of H-bonded boronic acids is substantial and its relevance at the solid state has been essentially limited to the self-associated architectures, data regarding the thermodynamics of the interactions with complementary recognition motifs in solution are essentially unknown. With the desire to explore the potentials of boronic acids as self-adapting H-bonding recognition molecular modules, the aim of this paper focuses on the study of the association capabilities of ArB(OH)₂ to form DD•AA type heterocomplexes, in which the H-bonding donor hydroxyl groups adopt a *syn-syn* conformation. This can be considered as a dynamic mimic of bicyclic guanidinium binding modules.¹⁹ Considering Jorgensen's model²⁰ on multiple H-bonding systems, the proposed DD•AA heteromolecular complexes should display enhanced stability as a consequence of the favorable secondary interactions. In identifying suitable complementary AA acceptors, we were drawn to 1,8-naphthyridine (**NAP**) that, with its N...N distance of 2.403 Å, structurally matches the conformational properties of *syn-syn* boronic acid (Scheme 1). In addition, its easy synthetic accessibility and the prospect to prepare an acceptor partner featuring multiple AA moieties (AA-AA), such as 5,6,11,12-tetraazaphenanthrene (**TANP**),^{21a} provides opportunities to further investigate discrete and polymeric architectures²² with suitably tailored boronic acid (Scheme 1), and thus the construction of supramolecular H-bonded architectures. Hence, we started with the examination of dimeric 1:1 (DD•AA) complexes involving *syn-syn* boronic acids and **NAP** (Scheme 1a). In particular, the successful detection and quantification of the complexation in solution and at the solid state was first complemented by computational predictions, and then experimentally proven. Reference studies with 1,10-phenanthroline (**Phen**) have been also described, showing a similar DD•AA complexation behavior, also in agreement with the literature report^{17h} describing heteromolecular dimeric complexes with 4-bromo-, 4-hydroxyl- and 3-methoxyphenylboronic acid. Furthermore, a series of crystal structures of trimeric 2:1 and 1:2 complexes (*i.e.*, DD•AA-AA•DD and AA•DD-DD•AA, respectively) were also obtained and examined (Scheme 1b), showing the versatility of the recognition motif to build defined supramolecules. Finally, the procedure leading to the formation of crystals of the first supramolecular H-bonded polymeric network, (AA-AA•DD-DD)_n, respectively involving a diboronic acid and a suitable ditopic acceptor is discussed (Scheme 1c).



Scheme 1. Schematic representation of the possible non-covalent complexes formed between mono- or ditopic boronic acids with H-bonding acceptors **NAP** or **TAMP**. Discrete (a) 1:1, (b) 2:1 and 1:2 complexes and a (c) supramolecular polymer. All boronic acids have been purchased beside molecule **7** that was prepared following literature protocol.^{21b}

RESULTS AND DISCUSSION

Computational modeling of the conformational properties of phenyl boronic acid and its aptitude to form DD-AA complexes. In the literature, the relative energies of the three conformations a boronic acid moiety can adopt have been calculated, revealing a minor energy difference between them ($< 1 \text{ kcal mol}^{-1}$). The first report based its theoretical calculations on the substrate where the substituent is a hydrogen atom²³ and this was later

followed by the phenyl boronic acid analogue.^{17h} In both cases, the *syn-anti* conformation is the most favourable, since the repulsion of the two positively charged hydrogen atoms is minimized. This is in accordance with the large number of crystal structures where the boronic acid moiety is self-interacting in a *syn-anti* fashion.¹⁰⁻¹⁵ In line with the abovementioned literature reports, through Density Functional Theory (DFT) calculations performed at the B3LYP/6-311G**level of theory, we also found that the *syn-anti* geometry is the most favourable conformation with respect to the *syn-syn* (-2.20 kcal mol⁻¹) and *anti-anti* (and -2.82 kcal mol⁻¹) arrangements for the phenyl boronic acid (Figure 2 upper panel). The low-ranked *anti-anti* conformation is also accompanied by a loss of planarity essentially caused by the steric hindrance occurring between the hydrogen atom of the hydroxyl groups and the *ortho*-H atoms of the phenyl ring (Figure 2). In order to gain information about the association capabilities with **NAP** with respect to the dimerization equilibrium between the single boronic acids, a comparative DFT theoretical analysis in *vacuum* was carried out. In particular, the theoretical estimation of the complexation enthalpy between the phenyl boronic acid and **NAP** was performed, considering the three conformational equilibria as well as the phenyl boronic acid homodimerization equilibrium as references. As shown in bottom panel of Figure 2, the homodimerization ($\Delta H = -15.31$ kcal mol⁻¹) of phenylboronic acid is not negligible if compared to the small energy difference between the three conformations. Nevertheless, the formation of the heterodimer is energetically favored ($\Delta H = -20.41$ kcal mol⁻¹) with respect to the DA•AD homodimer, supporting the idea for which the **NAP** scaffold is a suitable pre-organized H-bonding AA partner for forming DD•AA complexes with enhanced thermodynamic stabilities.

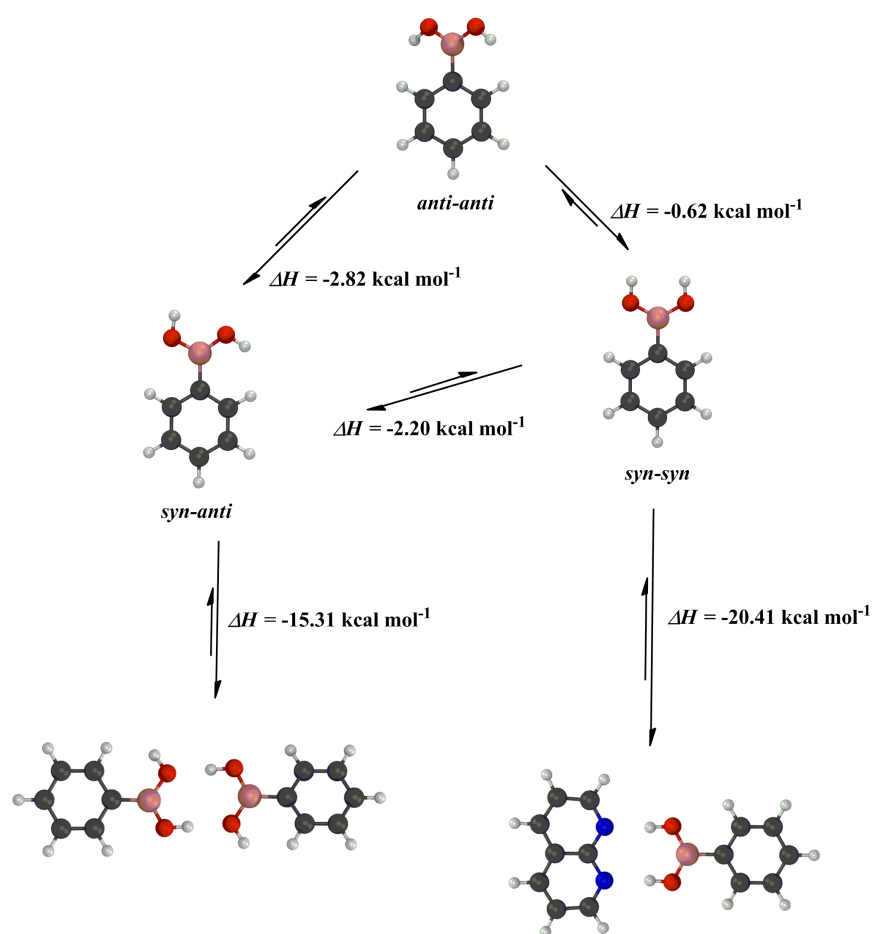
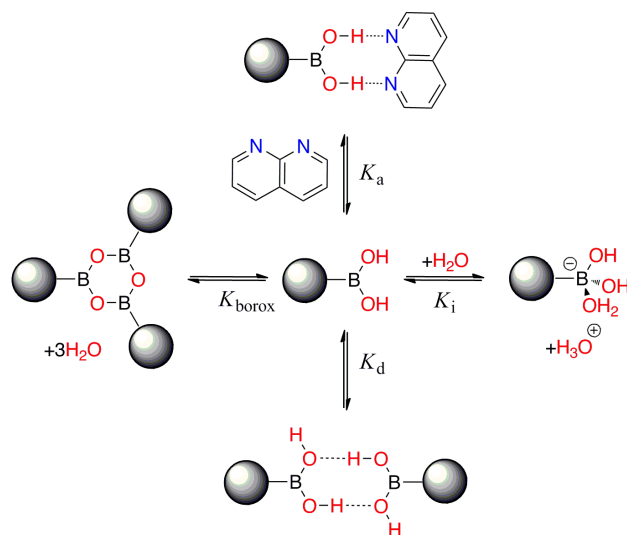


Figure 2. Calculated geometries and enthalpies for the three different conformations of phenylboronic acid (*i.e.*, *syn-syn*, *anti-anti*, *syn-anti*) and of the homo- and hetero-complexes (B3LYP/6-311G**, Gaussian 09). Red = oxygen, blue = nitrogen, pink = boron, white = hydrogen and black = carbon.

Determination of the heteromolecular association constant in solution (K_a) by NMR and ITC investigations.

Due to the fast hydrogen atom exchange that usually occurs in solution with acidic protons, the proton resonances of a boronic acid are usually not observed in most of the cases where CDCl₃ is used as solvent. Instead, when

Tol- d_8 is used, a sharp peak fingerprinting the acidic $\text{ArB}(\text{OH})_2$ protons appears between 3.5 and 4 ppm (Figure 3a). Prior to discuss of the heteromolecular binding results, a careful examination of the chosen experimental conditions revealed necessary, as aryl boronic acids can be involved in other equilibriums, beside that of the AA•DD complex (Scheme 2). In particular, boronic acids are known to be in equilibrium with their cyclic anhydride form, namely the boroxine (K_{borox}).²⁴ The equilibrium in solution between the acid and the anhydride forms, mainly depends on the temperature and on the position of the aryl substituents, with the derivatives bearing *ortho* substituents being kinetically more stable, exclusively existing as acids in solution at room temperature compared to the *para* analogues, which are often found as mixtures.^{1,24b} To avoid the presence of the boroxine form, only *ortho*-substituted $\text{ArB}(\text{OH})_2$ derivatives were thus used to estimate the homoassociation constants in solution (as one can see, the presence of the boroxine form can be easily diagnosed with ^1H -NMR picking the fingerprinting Ar-H resonances, Figure 3b). Next, the homodimerization constants (K_d) for the relevant boronic acids were also measured. Dilution experiments revealed K_d values lower than 10 M^{-1} in Tol- d_8 (see the dilution ^1H -NMR experiments in the SI), suggesting that the homodimerization equilibrium has a negligible effect on the heteroassociation with either **NAP** or **Phen**. This is in line with the literature reports describing other weakly H-bonded AD-DA type homodimers.²⁵ Finally, the effect of water was studied, as the formation of the hydroxyboronate ions (K_i) could affect the determination of the heteromolecular association due to the structural change of the functional group, namely from a trigonal planar and tetrahedral structure.²⁶ Although the addition of successive aliquots of H_2O did not show any appreciable change in the chemical shift of the boronic acid *OH* proton resonances in the ^1H -NMR spectrum taken in Tol- d_8 (see SI), it is known that a fast chemical exchange²⁷ between the trigonal boronic acid and tetrahedral hydroxyboronate ion is present. Given the nature of this fast equilibrium, the diagnostic ^{11}B and ^1H resonances fingerprinting the hydroxyboronate and the boronate groups under neutral pH conditions are not detected. However, considering that the ^{11}B resonances for all boronic acids investigated in this work are centered at ca. 30 ppm,^{27a} we cannot entirely exclude the presence of tetrahedral hydroxyboronate ions. Low-temperature ^1H -NMR experiments were also performed to investigate the existence of any H-bonding interactions between the boronic acid *OH* protons and the water molecules. Again, no direct evidences about any H-bonding interactions between these two molecules were observed (see SI). Hence, to ensure the same experimental conditions for the binding studies with the relevant boronic acids and acceptors, the ratio between the boronic acid and the H_2O content was kept constant in all solutions.



Scheme 2. Chemical equilibriums involving a boronic acid in solution: formation of a non-covalent AD-DA type homodimer (K_d) and DD-AA heterodimer (K_a), boroxine (K_{borox}) and hydroxyboronate ions (K_i).

Given these experimental premises, the H-bonding DD-type self-adaptability of aryl boronic acids toward the association with suitable AA acceptors (**NAP** or **Phen**) was systematically studied by considering different derivatives (listed in Table 1) for the first time through ^1H -NMR titration experiments. Titration experiments (Figure 4a and SI) showed a fast association equilibrium involving a progressive downfield shift of the diagnostic boronic acid *OH* resonances for all the derivatives (Table 1, **1-5**) upon incremental addition of **NAP** (for instance, the δ_H of the *OH* shifts from 3.77 to 9 ppm for the **1•NAP** complex, Figure 4a). Through a free-concentration nonlinear

least-squares curve-fitting²⁷, for which the initial concentration of the boronic acid is also considered as a variable (C_0'), the association constants (Table 1 and Figure 4b) were found to be 369 ± 16 , 997 ± 62 , 1465 ± 66 , 903 ± 41 and $6900 \pm 760 \text{ M}^{-1}$ for complexes **1•NAP**, **2•NAP**, **3•NAP**, **4•NAP** and **5•NAP**, respectively, all displaying a 1:1 stoichiometry (as evidenced by the Job plot analysis, see that of **1•NAP** in Figure 4c). If compared to other AA•DD complexes, the association values are in line with those reported in the literature.^{21c,29} As one can notice, the fitted C_0' is always lower than that supposed experimentally, namely $C_0 = 0.01 \text{ M}$. Likely, this is ascribed to the presence of the hydroxyboronate formation equilibrium (see discussion above), which significantly reduces the real concentration of the boronic acids in solution. Although 2,6-bis(trifluoromethyl)phenylboronic acids did not form any boroxine in toluene and only a 15% was observed for solutions containing 3,4,5-trifluorophenylboronic (estimated by ¹H-NMR through the aromatic proton resonance at 7.40 ppm), attempts to measure the association constants between these phenylboronic acids and **NAP** by NMR proved to be fruitless, as the peak fingerprinting the *OH* resonances becomes extremely broad during the titration experiments or overlaps with the solvent shift respectively, thus preventing an accurate estimation of the chemical shift values (see SI). Model titration experiments were also performed in other solvents (CD_2Cl_2 and CD_3CN) with boronic acid **3** and **NAP** the donor and acceptor molecules, respectively, to study the effect of the solvent polarity on the 1:1 association strength. As expected, solvents with increasing dielectric constants cause a progressive decreasing of the strength of the H-bonding interaction,³⁰ with the association constants $K_a(\text{solvent})$ being the following: 1465 ± 66 in toluene ($\epsilon = 2.38$), 1234 ± 54 in CD_2Cl_2 ($\epsilon = 8.93$) and 10.94 ± 0.48 in CD_3CN ($\epsilon = 37.5$).

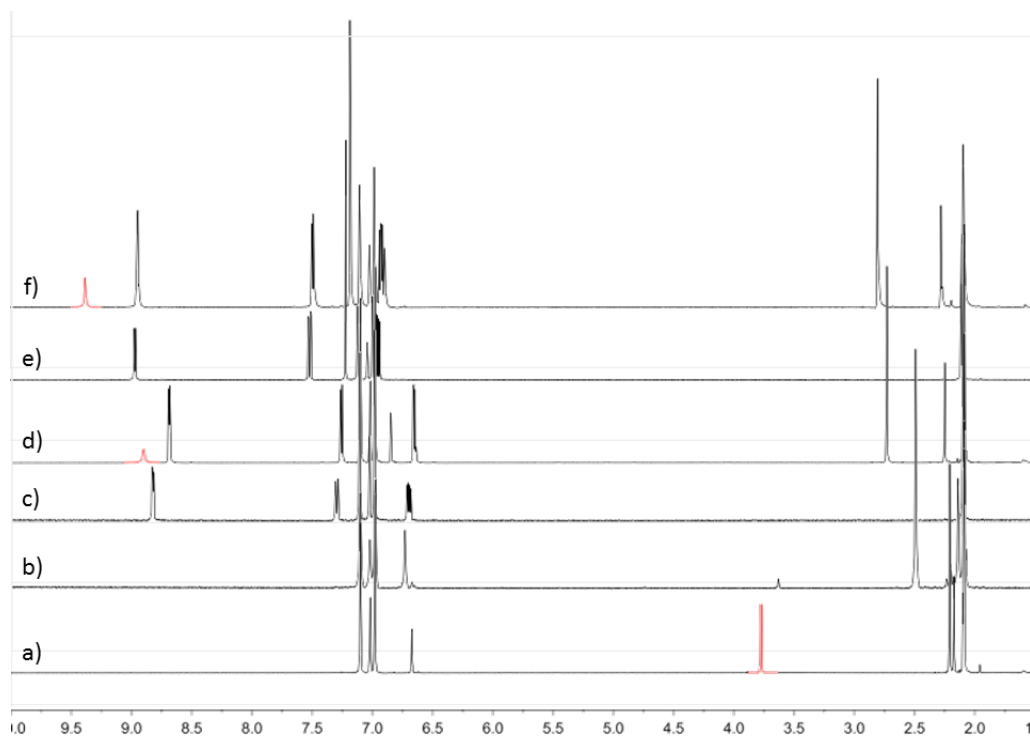


Figure 3. Selected region of ¹H NMR spectra (500 MHz, Tol-*d*₈, 298 K) of (a) mesitylboronic acid **1**, (b) mesitylboroxine, (c) **NAP**, (d) 1:1 **1•NAP** complex, (e) **Phen** and (f) 1:1 **1•Phen** complex.

Similar results were also obtained by complementary isothermal titration calorimetry (ITC) titrations, even if the values are approximately and systematically 20% lower than those measured by NMR. It is worth mentioning that, except for the **13•NAP** and **5•NAP** complexes, the affinity constants are in the lower range of values accessible by ITC and those could only be measured thanks to the high solubility of both the host and guest molecules in toluene. The trend observed in the K_a values is the same for both methods, *i.e.* an increased affinity for the boronic acid derivatives bearing electron-withdrawing groups. As expected, the increased affinity is predominantly of enthalpic origin, as confirmed by the ΔH° values reported in Table 1. Specifically, complex **1•NAP** displays the less favorable interaction enthalpy and affinity constant, whereas the most favorable values are obtained for complex **13•NAP**, which is the only complex not bearing *ortho*-substituents and the only one showing a ‘flat’ geometry. Reference titration experiments (see SI) with 2-methoxyphenylboronic acid **14**, in which the boronic

acid OH protons are preferentially locked in the *syn-anti* through an intramolecular H-bonding interaction established with the methoxy group, did not show any significant downfield shift of the OH resonances. This suggests that no complex is formed when the characteristic conformational dynamics of the boronic acid recognition group is lost.

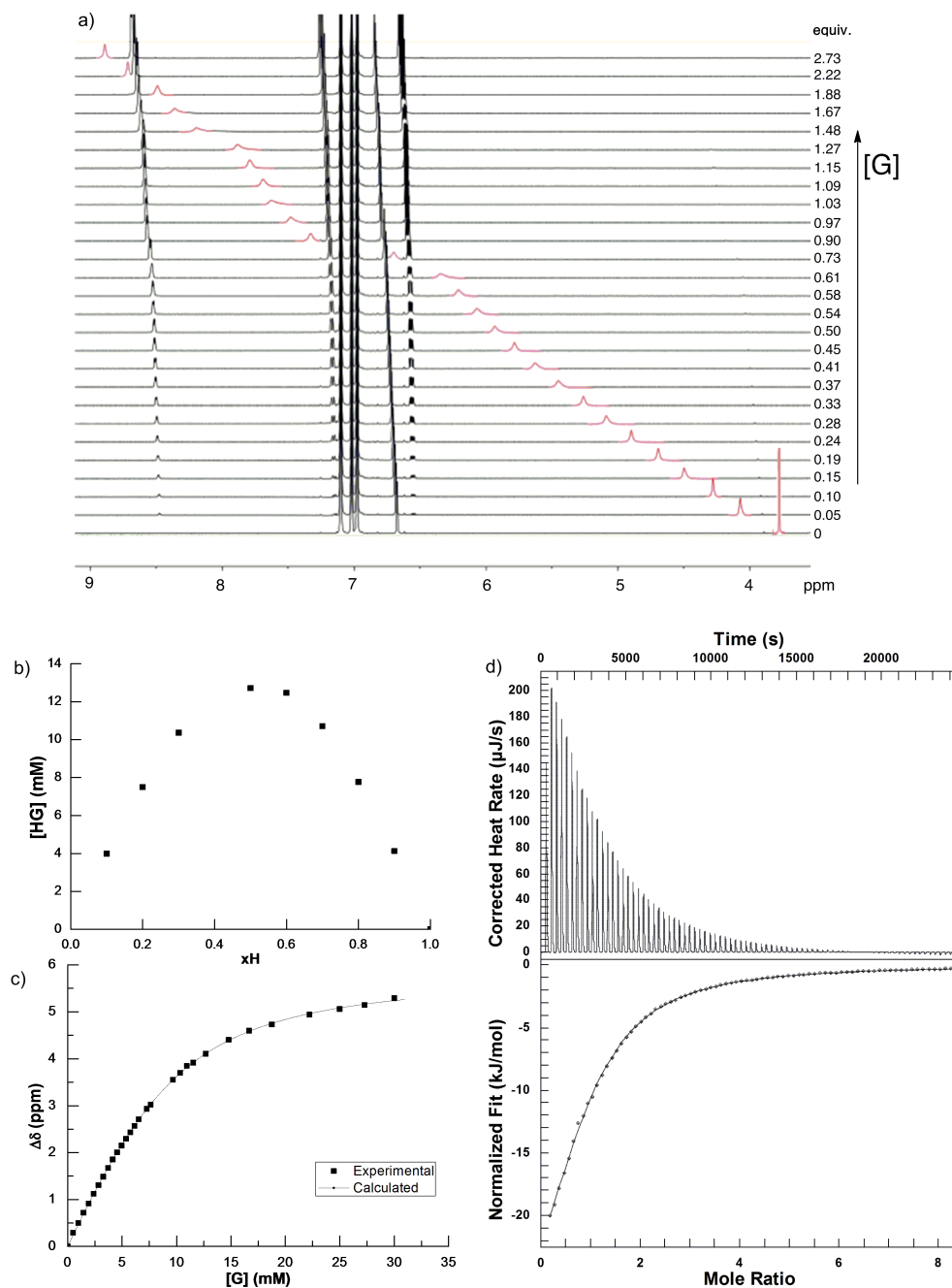
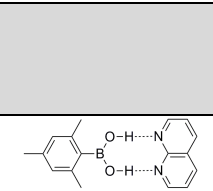
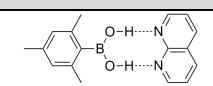
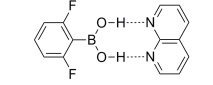
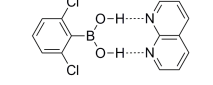
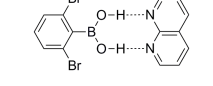
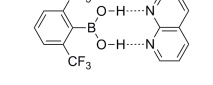
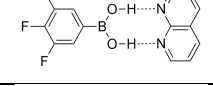
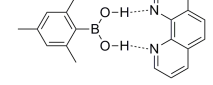
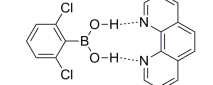


Figure 4. (a) Selected region of a series $^1\text{H-NMR}$ spectra acquired during the titration of boronic acid **1** with NAP (500 MHz, $\text{ToI-}d_8$, 298 K) with a concentration of the initial boronic acid being $C_0 = 0.01\text{ M}$; (b) binding isotherm for the formation of the 1:1 complex ($[\text{H}]_0 = [\mathbf{1}] = 10\text{ mM}$, $[\text{G}]_0 = [\text{NAP}] = 50\text{ mM}$, $\Delta\delta_{\text{sat}} = 5.23$, $K_a = 369 \pm 16$), (c) Job plot confirming the formation of the 1:1 $\mathbf{1}\cdot\text{NAP}$ complex ($[\text{H}]_0 + [\text{G}]_0 = 5\text{ mM}$, $xH = [\text{H}]_0 / ([\text{H}]_0 + [\text{G}]_0)$); (d) ITC data for the titration of boronic acid **1** (4.9 mM) with NAP (200mM) in toluene at 298 K.

Being able to determine the K_a of 1:1 molar ratio complexes, we also attempted to study in solution the formation of the trimeric complexes (Scheme 1b). Unfortunately, the scarce solubility of the ditopic molecular modules (*i.e.*, 1,4-diphenyleneboronic acid **17**, 2,5-thiophenediboronic acid **18** and 5,6,11,12-tetraazanaphthacene, **TANP**)

in toluene hampered an accurate determination of the thermodynamic properties of the involved equilibria. However, when CD_2Cl_2 is used, we could estimate the association strength of a boronic acid with TANP due to its solubility in chlorinated solvents. In particular, using boronic acid **3** as suitable DD molecular partner, a 1:2 association equilibrium could be probed with **TANP** acceptor. Two weak association constants were measured, K_{a1} (126 ± 2) and K_{a2} (29 ± 1), for the formation of the 1:1 (*i.e.*, **3•TANP**) and 1:2 (*i.e.*, **3•TANP•3**) complexes, respectively. The weak association strengths are not surprising given the low basicity of this kind of aromatic heterocycles. To our surprise, when the AA partner was changed to **Phen** a significant enhancement of the association constants for complexes **1•Phen** and **3•Phen** were observed (769 ± 35 and $4953 \pm 54 \text{ M}^{-1}$, respectively) if compared to the **NAP** (369 ± 12 and $1465 \pm 66 \text{ M}^{-1}$, respectively). A careful analysis of the computed electronic surface potential (ESP, see SI), suggests that the stronger association can be reasonably attributed to stronger favorable secondary electrostatic N \cdots H interactions, the latter strengthened by the closer interatomic N \cdots H distances given by the peculiar arrangement of the N atoms in the phenanthroline scaffold.

Table 1. Association constants (K_a) values determined by NMR and ITC for the relevant substituted aryl boronic acids to **NAP** and **Phen** in toluene- d_8 (295 K). Values obtained by NMR were calculated through a free-concentration fitting approach of a 1:1 binding isotherm, where the initial concentration of the boronic acid is also considered as a variable and it is calculated consequently (C_0'). Uncertainty in K_a was estimated from two/three independent runs. Thermodynamic parameters derived from ITC experiments represent the mean value of the values obtained by fitting of a 1:n binding isotherm to three independent experiments and the reported errors represent the 95% confidence interval.

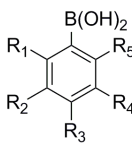
| Complex |  | K_a^a | $C_0'^b$ | K_a^a | ΔH^{0c} | $-T\Delta S^{0c}$ | n |
|---------------|---|----------------|----------|------------------|-----------------|-------------------|-----------------|
| | | NMR | | ITC | | | |
| 1•NAP |  | 369 ± 16 | 9.2 | 300 ± 60 | -8.9 ± 0.3 | 5.5 ± 0.5 | 0.95 ± 0.05 |
| 2•NAP |  | 997 ± 62 | 8.7 | 750 ± 100 | -10.5 ± 0.5 | 6.7 ± 0.5 | 1 ± 0.05 |
| 3•NAP |  | 1465 ± 66 | 8.7 | 1100 ± 200 | -11.7 ± 0.5 | 7.4 ± 0.5 | 0.97 ± 0.08 |
| 4•NAP |  | 903 ± 41 | 7.7 | 1700 ± 200 | -9.3 ± 0.3 | 5.0 ± 0.3 | 0.82 ± 0.04 |
| 5•NAP |  | 6900 ± 760 | 8.7 | 4600 ± 500 | -10.5 ± 0.5 | 6.7 ± 0.5 | 0.9 ± 0.1 |
| 13•NAP |  | - | - | 18000 ± 2500 | -11.7 ± 0.3 | 7.4 ± 0.5 | 1 ± 0.01 |
| 1•Phen |  | 769 ± 35 | 1.0 | _d) | _d) | _d) | _d) |
| 3•Phen |  | 2306 ± 79 | 8.8 | _d) | _d) | _d) | _d) |

^a M^{-1} . ^b mM. ^c kcal mol^{-1} . ^d) not measured.

Computational modeling of the structural and association energies of the DD•AA complexes. To shed further light on the electronic and conformational properties ruling the formation and the stability of the different heteromolecular complexes, DFT geometry optimization and frequency calculations were carried out in *vacuum*, at the B3LYP/6-311G** level using the Gaussian 09 (see SI-1). Starting from the reference phenylboronic acid (Table 2, acid **6**), it was confirmed that the *syn-anti* conformation results to be the most favored, with the *syn-syn*

at 2.2 kcal mol⁻¹ higher in energy adopting an ‘in-plane’ conformation with the phenyl ring, in contrast to the *anti-anti* conformation which is highest in energy and ‘out-of-plane’. A similar trend where the *syn-anti* > *syn-syn* > *anti-anti* ranking is noted in the cases of *para* substituted derivatives, bearing electron-withdrawing groups (EWGs, Table 2, acid **7**, **8** and **13**). On the other hand the stability ranking changes exerting the *anti-anti* as the second favored conformation after the *syn-anti* in derivatives **9**, **3** and **1**. Among these, derivatives **3** and **1** found a better accommodation in an ‘out-of-plane’ rotamer due to the steric hindrance of the substituents in both *ortho* positions. A small energy barrier of about 1.5 kcal mol⁻¹ exists between the *anti-anti* and the *syn-anti* conformations, while more considerable energy barriers have to be overcome to reach the *syn-syn* arrangement. Moving to the *ortho*-substituted derivatives **2** and **15**, it has been observed that the presence of other electron EWGs than chlorine, such as fluorine, lead to weak intramolecular H-bonds, with a OH...F distance of 1.95 Å, the latter stabilizing the *anti-anti* conformation as the most favored, although with a very low difference in energy (0.38 kcal mol⁻¹ more stable than the *syn-anti*). On the contrary, a considerable difference in energy is detected when the *syn* conformation has to be adopted (-5.84 kcal mol⁻¹). Most importantly, the enthalpy of dimerization was computed of all these derivatives in couple with **NAP**. In comparison with reference phenylboronic acid (Table 1, acid **6**), all derivatives showing the *syn-syn* conformation as the second most favored exert a consistent ΔH of interaction that ranges from about -20 to -22 kcal mol⁻¹. Interestingly, the poor stability of the *syn-syn* conformation observed in derivatives **9**, **3** and **1** does not affect their ability to form a stable complex together with the **NAP** counterpart, which instead exerts comparable affinity values to those of phenylboronic acid. Hence, despite the relative stability of the three conformations the phenylboronic acid derivatives can adopt, the formation of the heterocomplexes is never compromised, beside molecule **15** where the only the *anti-anti* conformation is present due to intramolecular H-bonds established with the *ortho*-methoxy substituents. To appraise the H-bond donating character, we used the electrostatic surface potential (ESP) localized on the acidic OH hydrogen atoms (Table 2). By changing the electronic properties of the substituents, variations of the ESP values were observed, with lower and higher values when electron-donating groups (EDGs) and EWGs are present, respectively.

Table 2. Theoretical calculations at the B3LYP/6-311G** level of theory for different phenylboronic acids derivatives bearing substituents in different positions: a) $\Delta\Delta H$ for the *syn-syn* and *anti-anti* conformations compared to the *syn-anti*, b) dipole moment (μ), c) electrostatic potential (ESP) value corresponded to the acidic hydrogen and d) ΔH for the formation of the AA-DD complex involving **NAP**; ‘in’ and ‘out’ stand for ‘in-plane’ or ‘out-of-plane’ conformation adopted by the boronic acid moiety with respect to the aromatic plane of the aryl ring.

| | # | Substituent | | | | | <i>syn-syn</i> | <i>anti-anti</i> | μ^b | ESP ^c | Heterodimer |
|---|-----------|----------------|----------------|----------------|----------------|----------------|--------------------|--------------------|---------|------------------|-------------|
| | | R ¹ | R ² | R ³ | R ⁴ | R ⁵ | $\Delta\Delta H^a$ | $\Delta\Delta H^a$ | | | |
|  | 6 | H | H | H | H | H | 2.20 (in) | 2.82 (out) | 2.44 | 125.50 | -20.41 |
| | 7 | H | H | OMe | H | H | 2.07 (in) | 2.82 (out) | 2.56 | 134.16 | -19.91 |
| | 8 | H | H | SMe | H | H | 2.01 (in) | 2.89 (out) | 3.57 | 131.77 | -20.41 |
| | 13 | H | F | F | F | H | 1.38 (in) | 3.99 (in) | 0.003 | 119.22 | -22.48 |
| | 9 | H | H | F | H | H | 1.81 (in) | 1.35 (out) | 3.96 | 136.17 | -20.95 |
| | 3 | Cl | H | H | H | Cl | 3.39 (out) | 1.69 (out) | 1.55 | 112.95 | -21.79 |
| | 1 | Me | H | Me | H | Me | 3.38 (out) | 1.32 (out) | 3.18 | 100.40 | -20.44 |
| | 2 | F | H | H | H | F | 5.84 (out) | -0.38 (in) | 2.09 | 122.36 | -21.59 |
| | 15 | OMe | H | H | H | OMe | 5.82 (out) | -3.26 (in) | 0.91 | 90.99 | -18.67 |

^a $\Delta\Delta H$ calculated compared to the *syn-anti* conformation in kcal mol⁻¹. ^b D. ^c kcal mol⁻¹. ^d ΔH calculated compared to the free-complex *syn-syn* conformation in kcal mol⁻¹.

Solid-state recognition and supramolecular organization. Aiming at studying the formation of the doubly H-bonded complexes also in the solid state, we have co-crystallized a large variety of aryl boronic acids with the selected H-bond acceptor partners, *i.e.* **NAP**, **Phen** and **TANP**. In this case, *ortho*- and *para*-substituted aryl boronic acids (**1-16**) were studied, along with the aryl bis(boronic acid) derivatives (**17** and **18**) to form oligomeric and polymeric structures with the relevant H-bond acceptor partner. As predicted by the theoretical simulations and suggested by the NMR investigations in solution, we expected the boronic acids to self-adapt in a *syn-syn* conformation forming ‘T-shape’ or ‘flat’ complexes depending on the presence or the absence of *ortho* substituents, respectively (Figure 5). Therefore, parameters such as the stoichiometry and geometry of the complex, the H-bond distance, and the dihedral angle between the complexed boronic acid moiety and the aryl ring will be the subject of discussion in this section. Notably, in all X-ray studies only the crystal structures of the heteromolecular complexes were observed and no crystals of the free acids or its boroxine forms were detected. Surprisingly, this was also the case for those boronic acids known to easily undergo anhydride formation, namely the *para* substituted derivatives.²³

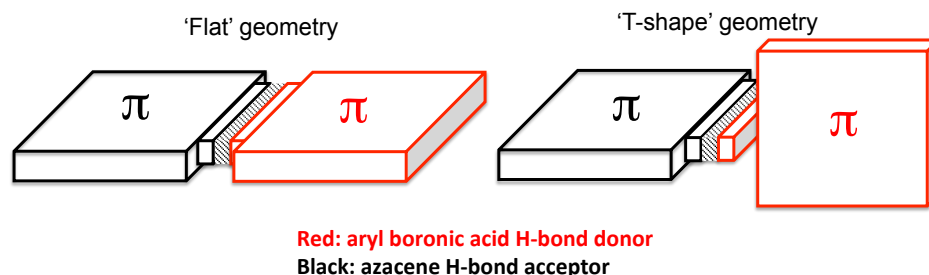


Figure 5. Representation of the ‘Flat’ and ‘T-shaped’ complexes.

Dimeric ‘Flat’ complexes. Co-crystallization of phenylboronic acid with **NAP** gave a 1:1 molar ratio dimeric complex (**6•NAP**) at the solid state (Figure 6a), where the N atoms are frontal to the O atoms. Being the two N atoms in the AA partner acting as H-bond acceptors the boronic acid moieties are suggested to adopt a *syn-syn* conformation thus yielding a pair of H-bonds with a distance of $N_2 \cdots O_2$ and $N_1 \cdots O_1$ 2.823 and 2.828 Å, respectively. In addition, the $B(OH)_2$ moiety is almost coplanar to the phenyl ring, since the torsion angle $O_1-B_1-C_1-C_6$ is only 3.9°.

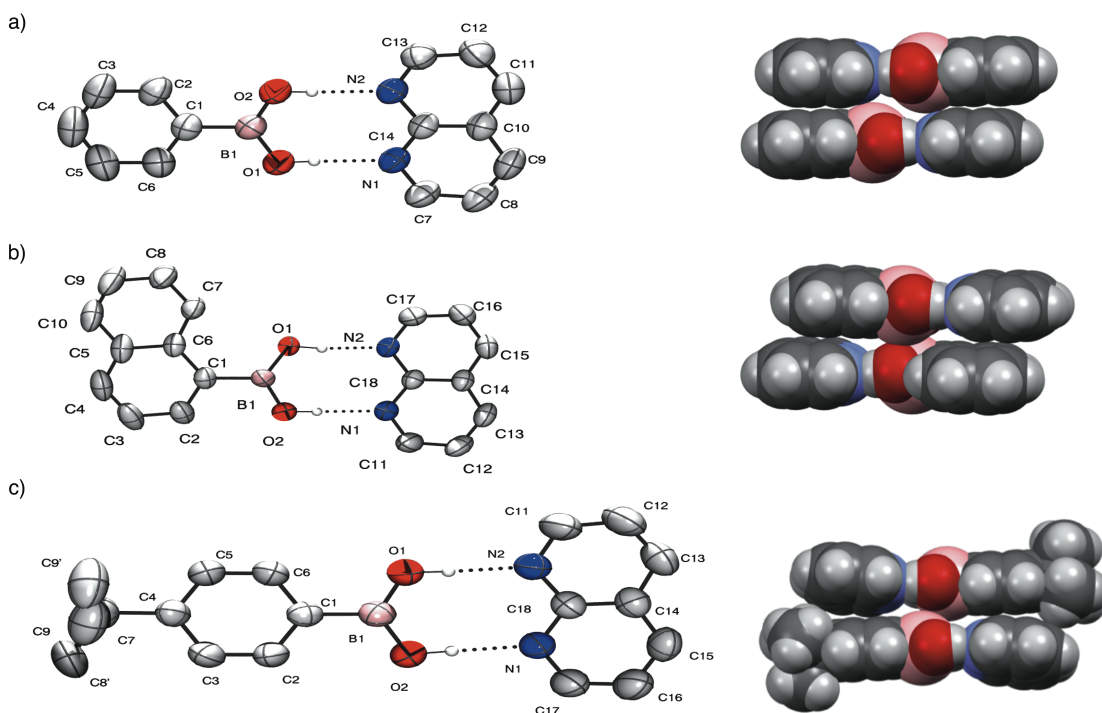


Figure 6. Crystal structures of the dimeric complex (a) **6•NAP**, (b) **16•NAP** and (c) **12•NAP**. Representation left: ORTEP (drawn at the 30% probability level) right: spacefill. Distances of the H-bonds: (a) $N_2 \cdots O_2$: 2.823(2) Å, $N_1 \cdots O_1$: 2.828(2) Å; (b) $N_2 \cdots O_1$: 2.792(3) Å, $N_1 \cdots O_2$: 2.833(4) Å and (c) $N_2 \cdots O_1$: 2.786(3) Å, $N_1 \cdots O_2$: 2.843(3) Å. Dihedral angle between the aryl and the boronic acid group: (a) $O_1-B_1-C_1-C_6$: 3.9(3)°, $O_1-B_1-C_1-C_2$: 2.6(3)°; (b) $O_1-B_1-C_1-C_6$: 3.5(4)°, $O_1-B_1-C_1-C_2$: 4.3(4)° and (c) $O_1-B_1-C_1-C_6$: 3.7(3)°, $O_1-B_1-C_1-C_2$: 4.6(3)°. Space group: (a) $P2_1/c$, (b) $P2_1/n$ and (c) $P2_1/c$.

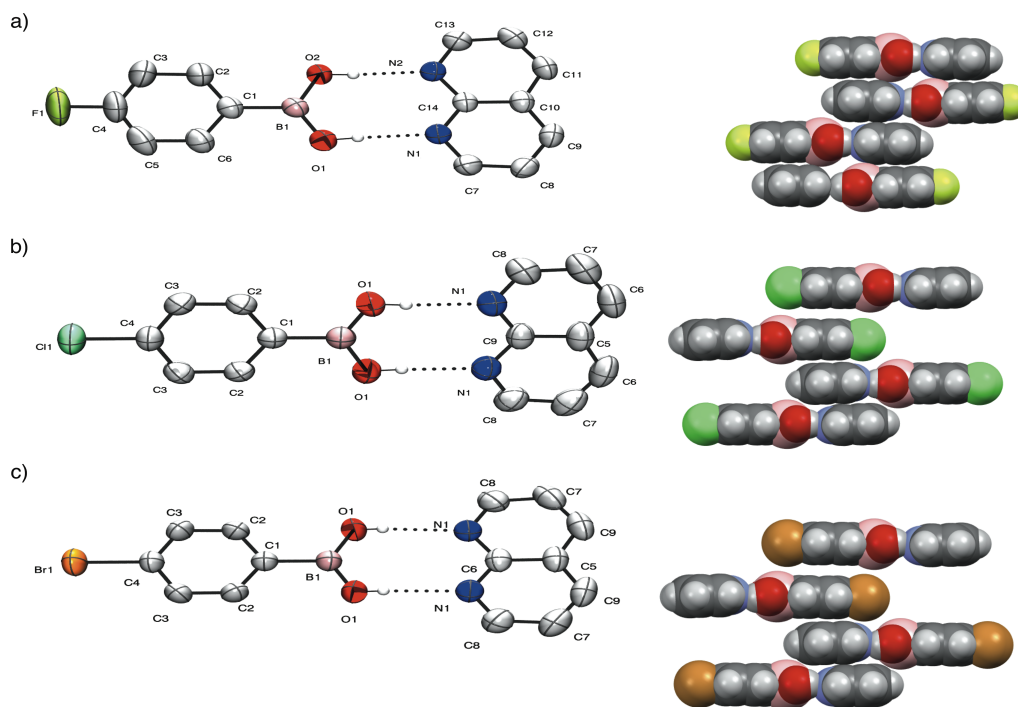


Figure 7. Crystal structures of the dimeric complex (a) **9•NAP**, (b) **10•NAP** and (c) **11•NAP**. Representation top: ORTEP (drawn at the 30% probability level) bottom: spacefill. Distances of the H-bonds: (a) $N_2 \cdots O_2$: 2.8250(19) Å, $N_1 \cdots O_1$: 2.8273(18) Å; (b) $N_1 \cdots O_1$: 2.825(2) Å and (c) $N_1 \cdots O_1$: 2.825(3) Å. Dihedral angle between the aryl and the boronic acid group: (a) $O_2-B_1-C_1-C_2$: 1.3(2)°, $O_1-B_1-C_1-C_6$: 0.93(2)°; (b) $O_1-B_1-C_1-C_2$: 0.5(3)° and (c) $O_1-B_1-C_1-C_2$: 0.8(6)°. Space group: (a) $P2_1/c$, (b) $C2/m$ and (c) $C2/m$.

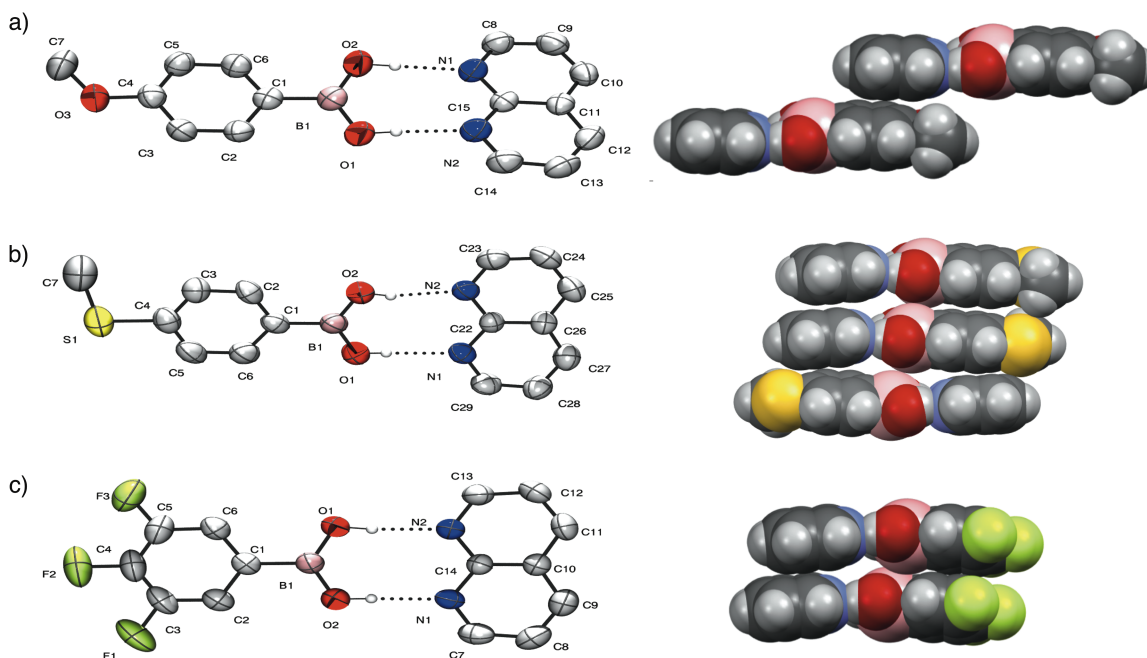


Figure 8. Crystal structures of the dimeric complex (a) **7•NAP**, (b) **8•NAP** and (c) **13•NAP**. Representation left: ORTEP (drawn at the 30% probability level); right: spacefill. Distances of the H-bonds: (a) $N_2 \cdots O_1$: 2.819(2) Å, $N_1 \cdots O_2$: 2.845(19) Å; (b) $N_1 \cdots O_1$: 2.837(4) Å, $N_2 \cdots O_2$: 2.811(5) Å and (c) $N_2 \cdots O_1$: 2.820(3) Å, $N_1 \cdots O_2$: 2.829(3) Å. Dihedral angle between the aryl and the boronic acid group: (a) $O_1-B_1-C_1-C_2$: 10.0(2)°, $O_2-B_1-C_1-C_6$: 8.1(2)°; (b) $O_1-B_1-C_1-C_6$: 1.9(7)°, $O_2-B_1-C_1-C_2$: 0.8(6)° and (c) $O_1-B_1-C_1-C_2$: 2.99(4)°, $O_2-B_1-C_1-C_6$: 2.5(4)°. Space group: (a) $P2_1/c$, (b) $Pbcn$ and (c) $P2_1/c$.

In the three dimensional arrangement the dimeric complexes are held together by π - π interactions, where each **NAP** antiparallely stacks on a phenyl ring (3.509 Å). Similar observations are noted in the case of naphthalene-1-boronic **16** and 4-*t*-butylphenylboronic acid **12** (Figures 6b-c), with the latter displaying a slightly higher π - π stacking distance (3.797 Å vs 3.546 Å) most likely caused by the presence of the hindering *para t*-butyl substituent.

To investigate further the effect of the *para* derivatization, co-crystals of a series of *para*-substituted boronic acids (**9-11**) were analyzed, beginning with the halogen-bearing analogues (Figure 7). When coming to compare the three halogenated analogues as shown in Figure 7, it can be easily noted the increase in the offset between two π -stacked dimeric units moving from the F-, to the Cl- and finally to the Br-substituted derivatives. Specifically, the π -stacked dimers display an offset of 1.40, 6.42 and 8.93 Å, respectively. A closer look reveals that non-covalent halogen-halogen interactions of type-I as described by *Desiraju* (*i.e.*, van der Waals interactions of the dispersion-repulsion type)³¹ are present in 4-chloro and 4-bromophenylboronic acids. In particular, in both cases, based on the geometrical C-X \cdots X angles being equal to 189.50°, the interaction is symmetrical. This can be attributed to the need to minimize the repulsion between the two interacting halogen atoms by interfacing the neutral region of their electrostatic potential surface. In addition, a shorter X \cdots X interaction distance is noted for the Cl \cdots Cl contact compared to that of Br \cdots Br (3.30 Å vs 3.40 Å), with both values being shorter than the sum of the van der Waals radii of the relevant halogen atom.

Moving on to the *para* methoxy-substituted phenyl boronic acid **7**, a large offset is observed, *i.e.* 9.32 Å (Figure 8a). In contrast, the thiomethyl analogue **8** is characterized by the placement of the dimeric units both in a parallel and antiparallel manner, the first being driven by weak secondary bonding S \cdots S interactions. A similar behavior is noted for the co-crystals obtained for 3,4,5-trifluorophenylboronic **13**, which showed local segregation of the hydrogen and fluoride atoms. This drives the formation of a columnar π -stacking arrangement, in which the molecules are organized in a parallel fashion.

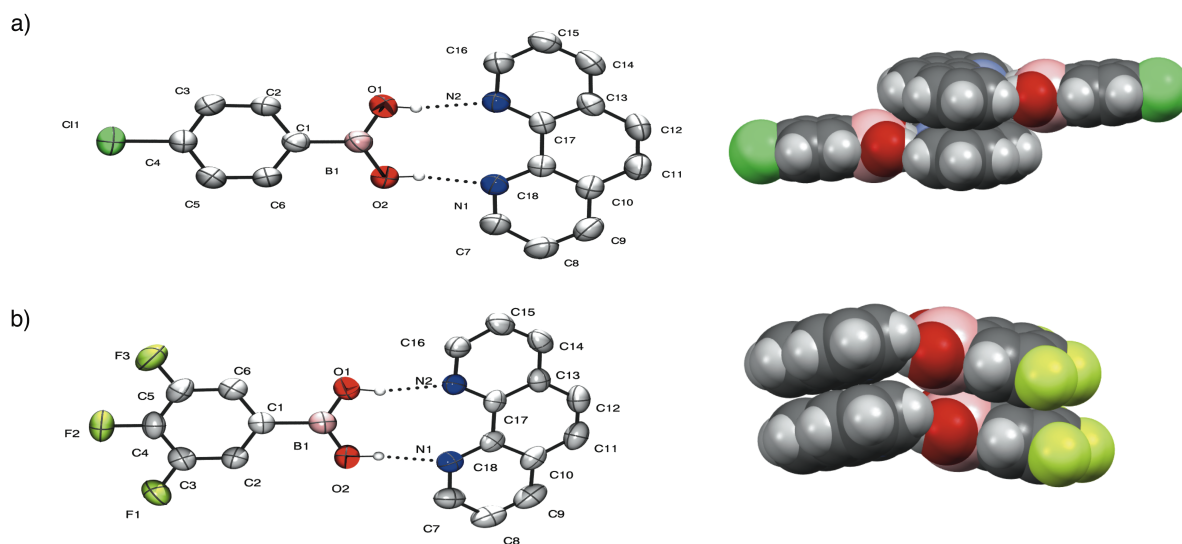


Figure 9. Crystal structures of the dimeric complex (a) **10•Phen** and (b) **13•Phen**. Representation left: ORTEP (drawn at the 30% probability level) right: spacefill. Distances of the H-bonds: (a) $N_2 \cdots O_1$: 2.834(2) Å, $N_1 \cdots O_2$: 2.750(2) Å and (b) $N_1 \cdots O_2$: 2.791(4) Å, $N_2 \cdots O_1$: 2.801(4) Å. Dihedral angle between the aryl and the boronic acid group: (a) $O_1-B_1-C_1-C_2$: 1.9(3)°, $O_2-B_1-C_1-C_6$: 3.40(3)° and (b) $O_1-B_1-C_1-C_6$: 3.8(5)°, $O_2-B_1-C_1-C_2$: 0.9(5)°. Space group: (a) $P1$ and (b) $P2_1/c$.

Similarly, the complexation at the solid state was also investigated with some selected arylboronic acids in the presence of **Phen** as acceptor. As shown in Figure 9, the molecular arrangements for the complexes of 4-chloro-**10** and 3,4,5-trifluorophenylboronic acid **13** with **Phen** are very similar to those obtained using **NAP** (Figures 6-8). The *syn-syn* conformation is indeed adopted triggering the interaction with the AA moiety of **Phen** though shorter H-bonding distances as compared to that observed with **NAP** (for example boronic acid **13** displays 2.791 Å vs 2.820 Å H-bonds distances with **Phen** and **NAP**, respectively for). This nicely reflects the solution NMR experiments, which indeed revealed stronger associations when phenylboronic acid derivatives are complexed with the **Phen** moiety.

Dimeric 'T-shaped' complexes. A pair of H-bonds was also identified at the solid state for the co-crystal obtained between bis-*ortho* substituted phenylboronic acids and **NAP** (Figure 10). In contrast to the above examples, the presence of the sterically hindering *ortho* substituents triggers the rotation of the boronic acid functional group with respect to the plane of the aryl ring upon formation of the non-covalent complex. This ultimately leads to the formation of complexes featuring a 'T-shaped' geometry, for which the planes of the two aromatic scaffolds are lying on different axes.

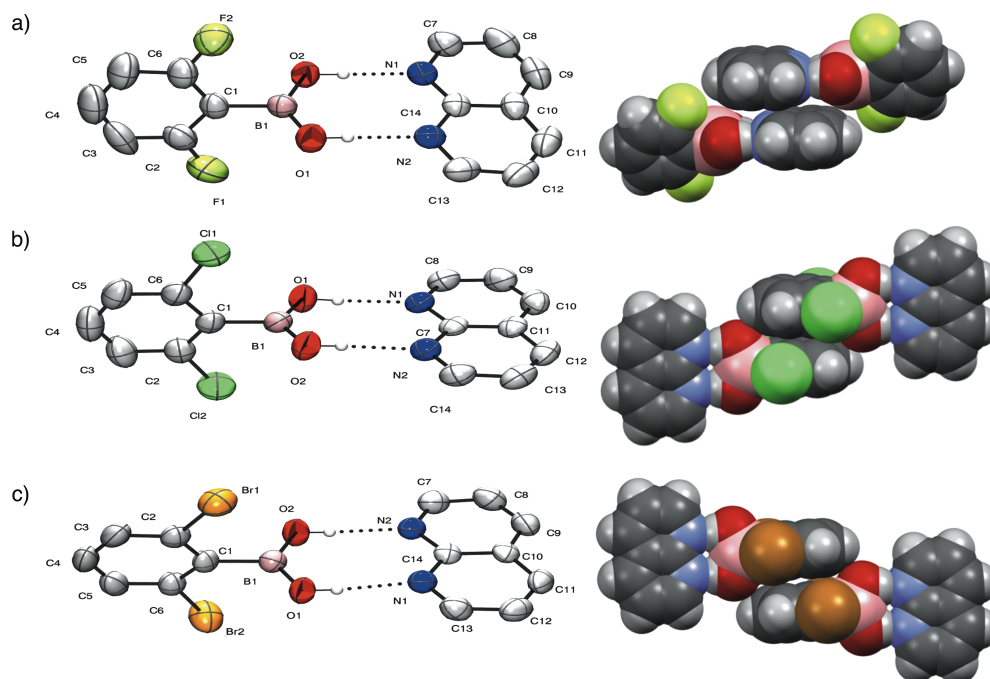


Figure 10. Crystal structures of the dimeric complex (a) **2•NAP**, (b) **3•NAP** and (c) **4•NAP**. Representation left: ORTEP (drawn at the 30% probability level) right: spacefill. Heteroatom distances for the H-bonds: (a) $N_2 \cdots O_1$: 2.798(2) Å, $N_1 \cdots O_2$: 2.7862(19) Å; (b) $N_2 \cdots O_2$: 2.802(2) Å, $N_1 \cdots O_1$: 2.812(2) Å and (c) $N_1 \cdots O_1$: 2.830(4) Å, $N_2 \cdots O_2$: 2.795(4) Å. Dihedral angle between the aryl and the boronic acid group: (a) $O_1-B_1-C_1-C_2$: 62.7(3)°, $O_2-B_1-C_1-C_6$: 62.4(5)°; (b) $O_1-B_1-C_1-C_2$: 89.4(2)°, $O_2-B_1-C_1-C_6$: 88.7(2)° and (c) $O_1-B_1-C_1-C_2$: 91.2(5)°, $O_2-B_1-C_1-C_6$: 90.3(5)°. Space groups: (a-c) $P2_1/c$.

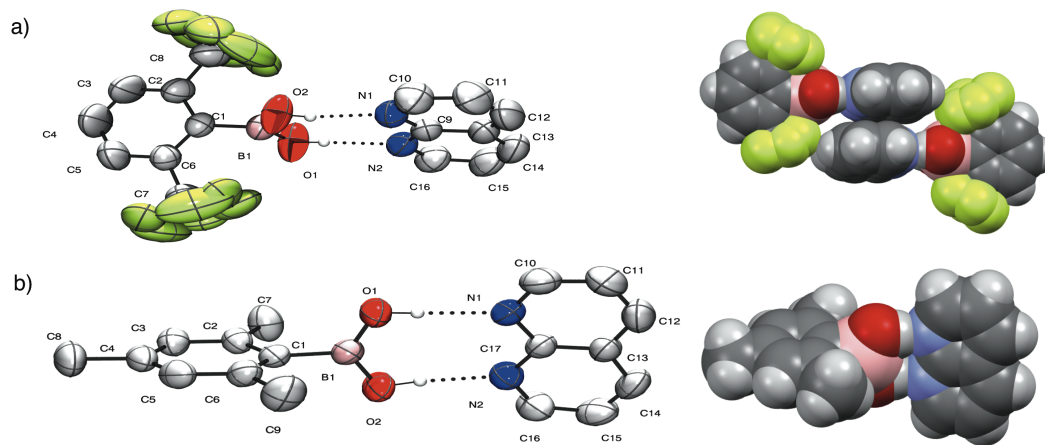


Figure 11. Crystal structures of the dimeric complex (a) **5•NAP** and (b) **1•NAP**. Representation top: ORTEP (drawn at the 30% probability level) bottom: spacefill. Distances of the H-bonds: (a) $N_2 \cdots O_1$: 2.796(2) Å, $N_1 \cdots O_2$: 2.803(2) Å and (b) $N_1 \cdots O_1$: 2.839(3) Å, $N_2 \cdots O_2$: 2.878(2) Å. Dihedral angle between the aryl and the boronic acid group: (a) $O_1-B_1-C_1-C_6$: 81.3(3)°, $O_2-B_1-C_1-C_2$: 84.4(3)° and (b) $O_1-B_1-C_1-C_6$: 89.6(3)°, $O_1-B_1-C_1-C_6$: 88.1(3)°. Space group: (a) $P2_1/n$ and (b) $P2_1/c$.

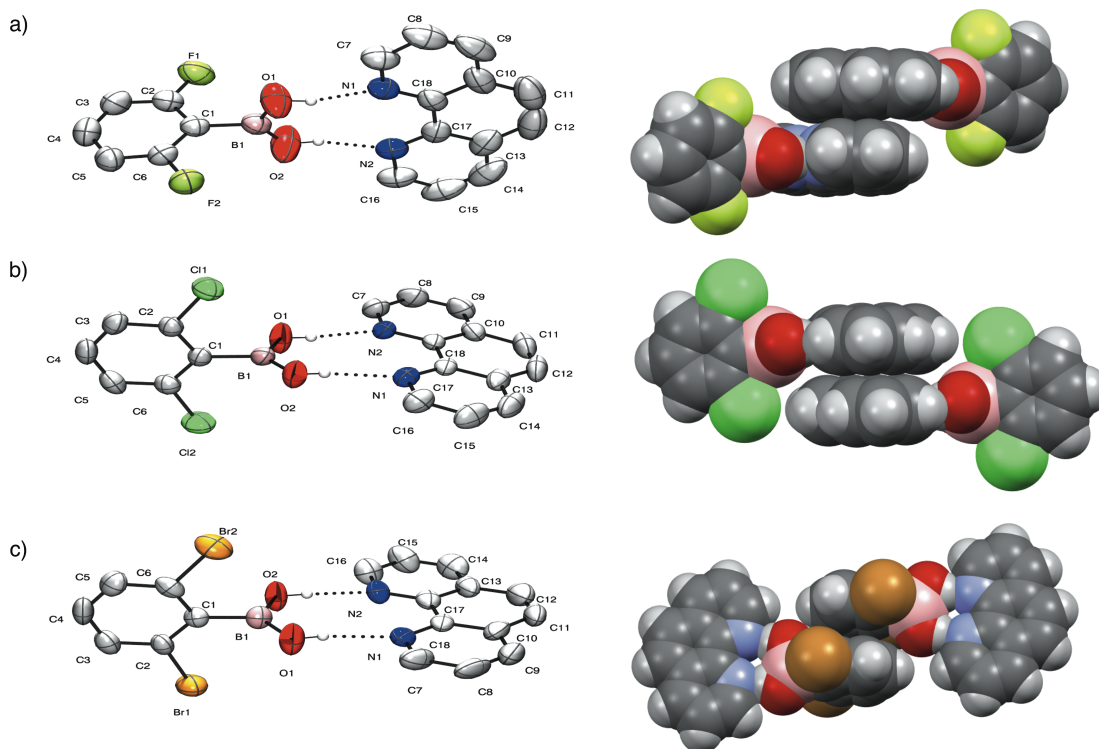


Figure 12. Crystal structures of the dimeric complex (a) **2•Phen**, (b) **3•Phen** and (c) **4•Phen**. Representation left: ORTEP (drawn at the 30% probability level) right: spacefill. Distances of the H-bonds: (a) $N_1 \cdots O_1$: 2.732(3) Å, $N_2 \cdots O_2$: 2.749(4) Å; (b) $N_2 \cdots O_1$: 2.767(2) Å, $N_1 \cdots O_2$: 2.815(2) Å and (c) $N_1 \cdots O_1$: 2.799(7) Å, $N_2 \cdots O_2$: 2.765(7) Å. Dihedral angle between the aryl and the boronic acid group: (a) $O_1-B_1-C_1-C_2$: 86.8(3)°, $O_2-B_1-C_1-C_6$: 88.6(4)°; (b) $O_1-B_1-C_1-C_6$: 83.7(2)°, $O_2-B_1-C_1-C_2$: 91.1(2)° and (c) $O_1-B_1-C_1-C_6$: 95.6(8)°, $O_2-B_1-C_1-C_2$: 88.9(8)°. Space group: (a) $P2_1/n$, (b-c) $P2_1/c$.

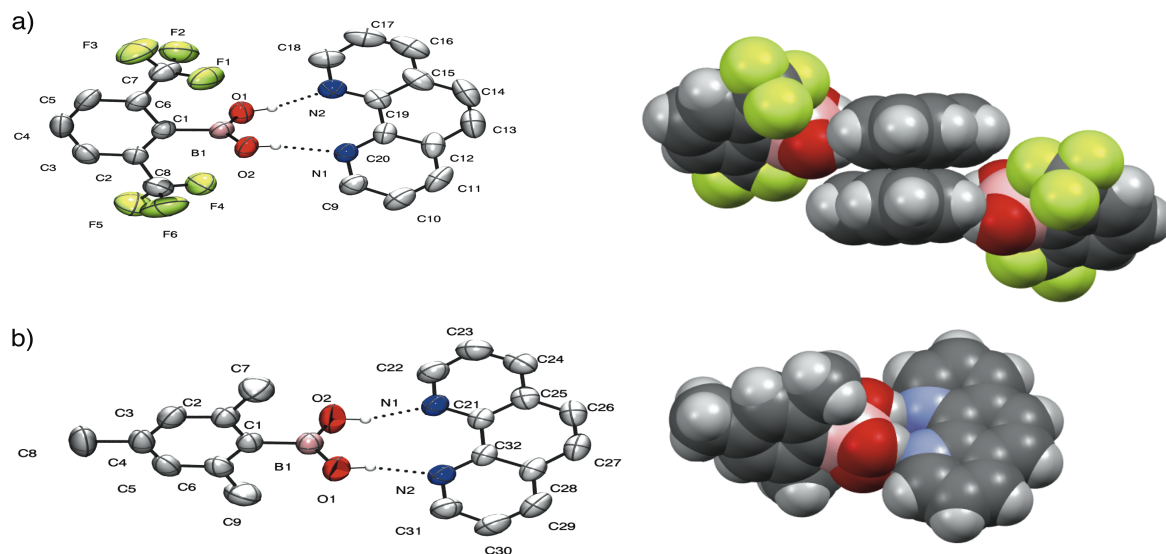


Figure 13. Crystal structures of the dimeric complex (a) **5•Phen** and (b) **1•Phen**. Representation left: ORTEP (drawn at the 30% probability level) right: spacefill. Distances of the H-bonds: (a) $N_2 \cdots O_1$: 2.772(4) Å, $N_1 \cdots O_2$: 2.787(3) Å and (b) $N_2 \cdots O_1$: 2.796(6) Å, $N_1 \cdots O_2$: 2.858(8) Å. Dihedral angle between the aryl and the boronic acid group: (a) $O_1-B_1-C_1-C_6$: 73.1(4)°, $O_2-B_1-C_1-C_2$: 77.8(4)° and (b) $O_1-B_1-C_1-C_6$: 54.3(4)°, $O_2-B_1-C_1-C_2$: 921(4)°. Space group: (a) $P2_1/c$ and (b) $P2/c$.

Starting with 2,6-difluorophenylboronic acid **2**, shorter H-bond distances (2.786 and 2.798 Å Figure 10a) are observed with respect to phenylboronic acid (2.823 and 2.828 Å, Figure 6a). The boronic acid distortion features here a dihedral angle $O_1-B_1-C_1-C_6$ of 62.7°, while the packing of the dimeric units is characterized by the antiparallel stacking of the **NAP** modules of two **2•NAP** complexes through π - π interactions (3.354 Å). Likewise in the case of 2,6-dichloro and 2,6-dibromophenylboronic acids (**2** and **3**), the torsion angle is almost 90°, induced by the presence of the larger *ortho* substituents (Figures 10b-c). An analogous trend can be observed for 2,6-bis(trifluoromethyl)phenylboronic acid **5** while for mesitylboronic acid **1**, the increased steric hindrance of its substituents impede the formation of strong π - π interactions between two neighboring complexes (Figure 11). The absence of π - π stacking was also observed when *ortho* substituted phenylboronic acids were co-crystallized with **Phen** (Figure 12 and 13). The halogen *ortho* disubstituted analogues display smaller H-bond distances with respect to the dimeric complexes with **NAP** (*i.e.* 2.767 Å vs 2.802 Å for 2,6-dichlorophenylboronic acid). Again, this is in agreement with the solution studies, which featured higher association strength with **Phen**. Similarly, the $-B(OH)_2$ twists perpendicularly to the aromatic ring to overcome the steric repulsion with the boronic acid functional group.

Trimeric complexes and crystal self-sorting. Further investigating the versatility of boronic acids to act as adaptable H-bonding tools in molecular recognition, a diboronic acid was attempted in a 1:2 complex by exploring multiple DD functionalities, DD-DD, interacting with two AA molecules (Figure 14). By evaporation of a 1:1 solution of 1,4-phenylenediboronic acid and **NAP**, a planar 1:2 complex (**NAP•17•NAP**) was successfully achieved stabilized by parallel π - π stacks between the aryl and **NAP** moieties with a distance of 3.502 Å and 3.480 Å, respectively (Figure 14a). Additionally, lateral diboronic acid derivatives come into play within the heteromolecular complex by creating a homomolecular branched network by means of lateral OH-H contacts (Figure 14a). A 1:2 complex (**NAP•18•NAP**) is also attained when 2,5-thiophenediboronic acid **18** is used (Figure 14b), yet no π - π stacking neither additional bridging H-bonding interactions could be observed in the crystal structure.

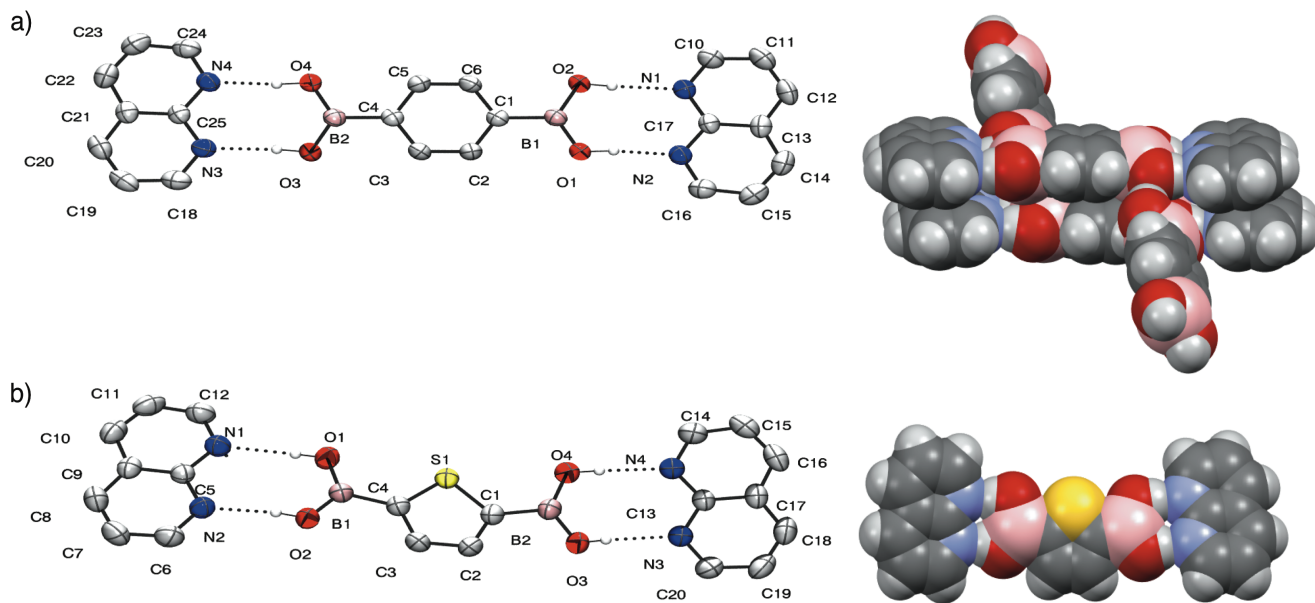


Figure 14. Crystal structures of trimeric complexes (a) **NAP•17•NAP** and (b) **NAP•18•NAP**. Representation left: ORTEP (drawn at the 30% probability level) right: spacefill. Distances of the H-bonds: (a) $N_1 \cdots O_2$: 2.8736(16) Å, $N_2 \cdots O_1$: 2.7420(16) Å, $N_3 \cdots O_3$: 2.8766(16) Å, $N_4 \cdots O_4$: 2.7527(16) Å and (b) $N_1 \cdots O_1$: 2.889(2) Å, $N_2 \cdots O_2$: 2.759(2) Å, $N_3 \cdots O_3$: 2.832(2) Å, $N_4 \cdots O_4$: 2.825(2) Å. Dihedral angle between the aryl and the boronic acid group: (a) $O_1-B_1-C_1-C_2$: 1.3 (2) $^\circ$, $O_2-B_1-C_1-C_6$: 0.7 (2) $^\circ$, $O_3-B_2-C_4-C_3$: 12.7 (2) $^\circ$, $O_4-B_2-C_4-C_5$: 9.4 (2) $^\circ$ and (b) $O_1-B_1-C_4-S_1$: 1.8(3) $^\circ$, $O_2-B_1-C_4-C_3$: 5.8 (3) $^\circ$, $O_3-B_2-C_1-C_2$: 17.2 (3) $^\circ$, $O_4-B_2-C_1-S_1$: 15.2 (3) $^\circ$. Space group: (a) P-1 and (b) P2₁/c.

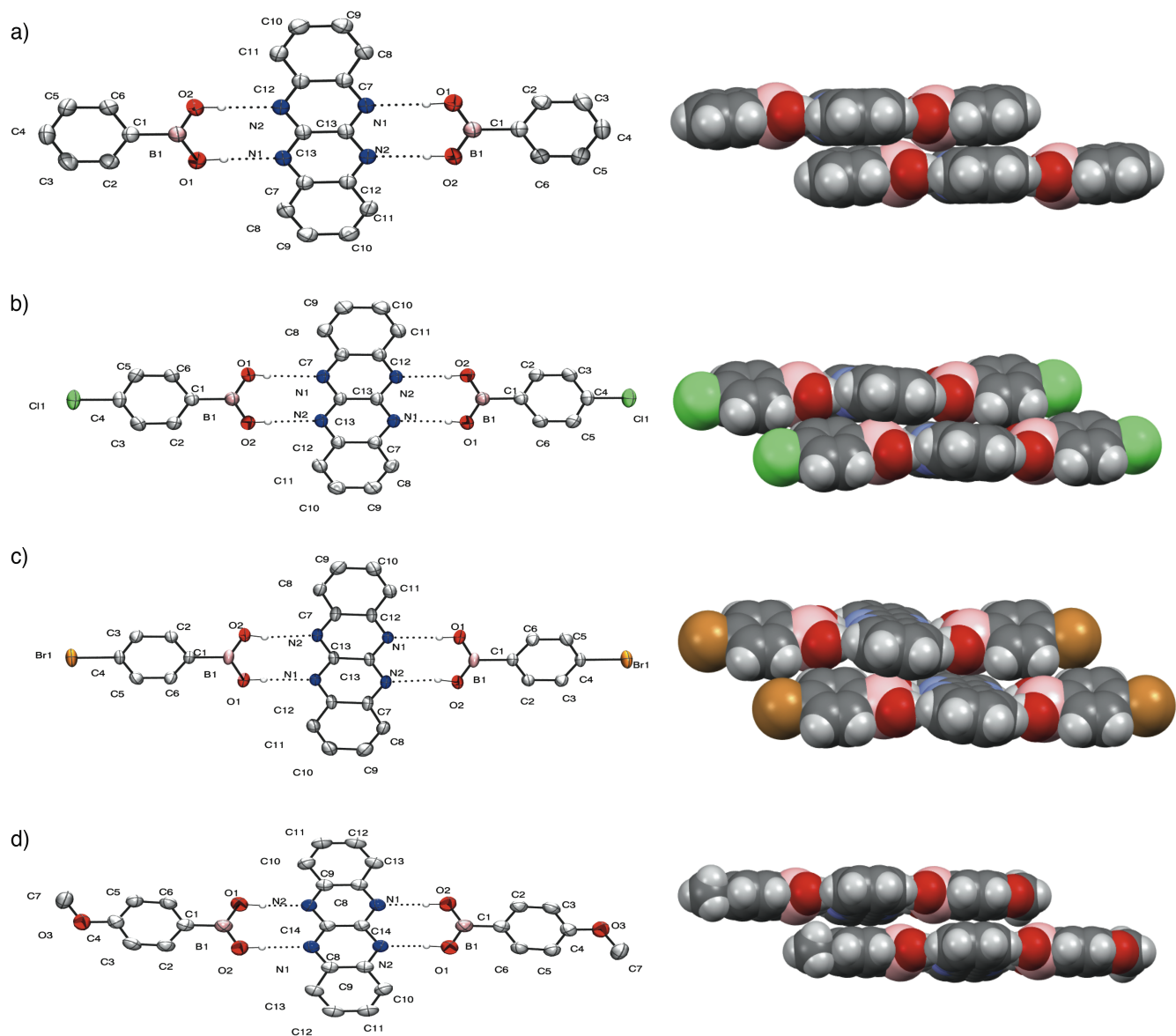


Figure 15. Crystal structures of trimeric complexes: a) **6•TANP•6**, (b) **10•TANP•10**, (c) **11•TANP•11** and (d) **7•TANP•7**. Representation left: ORTEP (drawn at the 30% probability level) right: spacefill. Distances of the H-bonds: (a) $N_2 \cdots O_2$: 2.882(4) Å, $N_1 \cdots O_1$: 2.908(4) Å; (b) $N_1 \cdots O_1$: 2.9031(15) Å, $N_2 \cdots O_2$: 2.9261(15) Å, (c) $N_1 \cdots O_1$: 2.892(5) Å, $N_2 \cdots O_2$: 2.952(5) Å and (d) $N_1 \cdots O_2$: 2.921(3) Å, $N_2 \cdots O_1$: 2.864(3) Å. Dihedral angle between the aryl and the boronic acid group: (a) $O_2-B_1-C_1-C_6$: 3.9(7)°, $O_1-B_1-C_1-C_2$: 5.0(8)°; (b) $O_2-B_1-C_1-C_2$: 15.5(2)°, $O_1-B_1-C_1-C_6$: 13.9(2)°, (c) $O_2-B_1-C_1-C_2$: 15.4(8)°, $O_1-B_1-C_1-C_6$: 14.9(8)° and (d) $O_2-B_1-C_1-C_2$: 3.6(4)°, $O_1-B_1-C_1-C_6$: 4.0(4)°. Space group: (a) P-1, (b) P-1, (c) P-1 and (d) P2₁/n.

On one hand monophenylboronic acid derivatives were also explored for the interaction in a 2:1 ratio by incorporating as a partner a ditopic AA-AA H-bond acceptor. Aiming at this, the AA-AA counterpart **TANP** was synthesized according to the literature procedure,³² then co-crystallized with a variety of aromatic-based boronic acids (*i.e.*, molecules **1**, **3**, **6**, **7**, **10**, **11** and **16**). The formation of single crystals was achieved by slow evaporation of toluene and the resulting trimeric complexes were successfully obtained in all the cases as outlined in Figure 16. As already observed so far, the presence of sterically bulky *ortho* substituents induces the formation of T-shaped complexes, as observed for trimeric complex **3•TANP•3** (Figure 16a). On the other hand, consistently with the dimeric flatten complexes, also in this case the $-B(OH)_2$ moiety adopts an in-plane conformation with the aromatic ring with 4-methoxyphenyl- and phenylboronic acids (complexes **6•TANP•6** and **7•TANP•7**). Notably, shorter H-bond distances, *i.e.* weaker H-bonding interactions, are observed going from 2:1, 1:2 to 1:1 complexes.

In fact, taking as example complexes including unsubstituted phenylboronic acids (**6** and **17**), the average H-bond distance ranges from 2.825 Å, 2.875 Å and 2.895 Å for complexes **6**•**NAP** (1:1), **NAP**•**17**•**NAP** (2:1) and **3**•**TANP**•**3** (1:2).

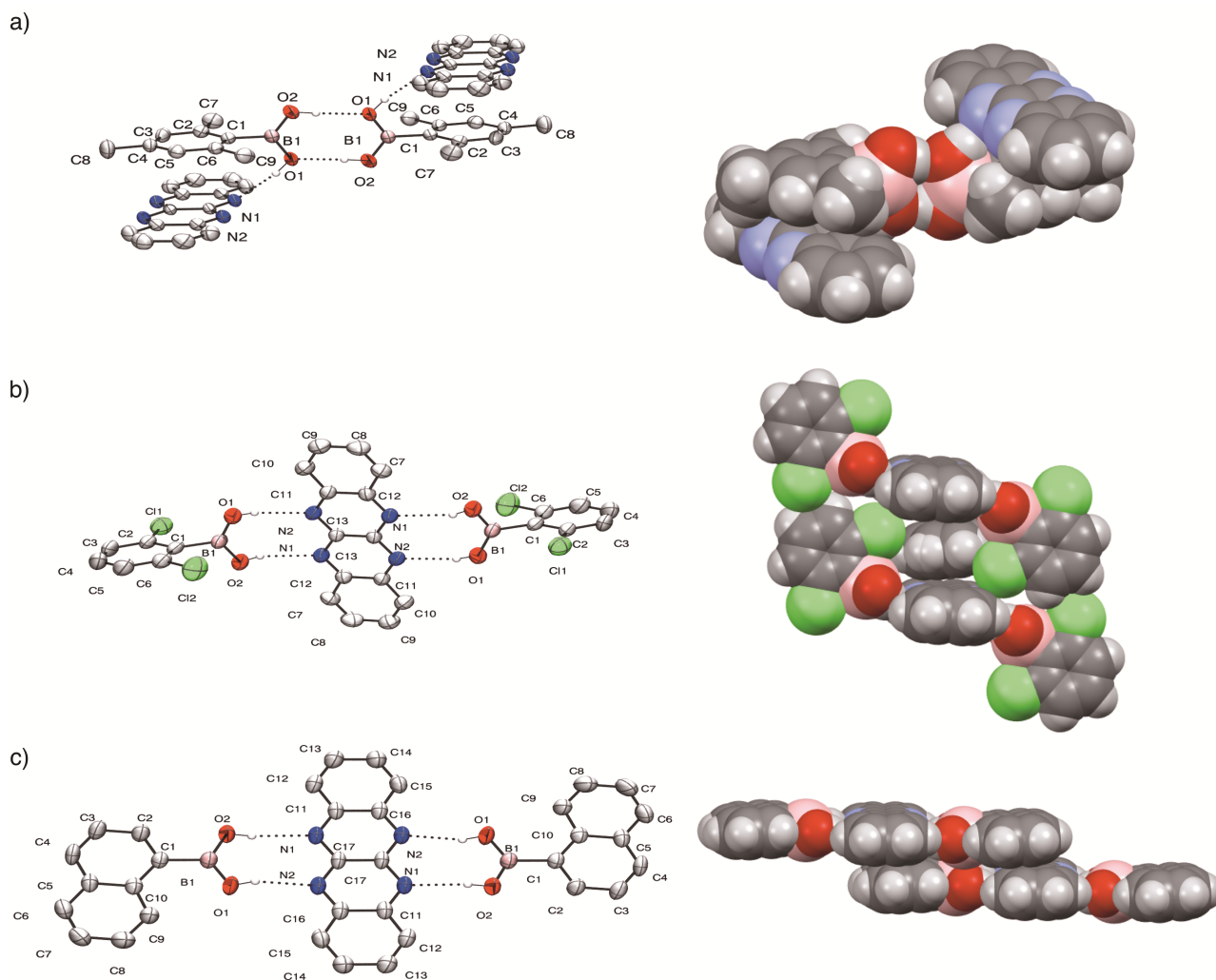


Figure 16. Crystal structures of trimeric complexes (a) **3**•**TANP**•**3**, (b) **1**•**TANP**•**1** and (c) **16**•**TANP**•**16**. Representation top: ORTEP (drawn at the 30% probability level) bottom: spacefill. Distances of the H-bonds: (a) $N_2 \cdots O_1$: 2.865(4) Å, $N_1 \cdots O_2$: 2.914(4) Å; (b) $O_1 \cdots O_2$: 2.831(3) Å, $N_1 \cdots O_1$: 2.945(2) Å and (c) $N_2 \cdots O_1$: 2.876(2) Å, $N_1 \cdots O_2$: 2.937(2) Å. Dihedral angle between the aryl and the boronic acid group: (a) O_2 - B_1 - C_1 - C_2 : 91.7(4)°, O_1 - B_1 - C_1 - C_6 : 90.8(4)°; (b) O_2 - B_1 - C_1 - C_6 : 92.6(2)°, O_1 - B_1 - C_1 - C_2 : 91.0(2)° and (c) O_2 - B_1 - C_1 - C_2 : 3.1(3)°, O_1 - B_1 - C_1 - C_6 : 2.8(3)°. Space group: (a) $P2_1/n$, (b) $P-1$ and (c) $P-1$.

Unexpectedly, sterically demanding mesitylboronic acid co-crystallizes adopting a *syn-anti* conformation, thereby forming a homomolecular dimer (Figure 16a). The **TANP** module finds now packing motif by entertaining π - π interactions with the aromatic portion of the mesitylboronic acid, additionally interacting through H-bonds with its *anti* B-OH proton (Figure 16a). This is enhanced from the crystal structures of 2,6-dichlorophenyl and naphthalene-1-boronic acid. In both structures the 1:2 trimeric complex is noted, but toluene is also co-crystallizing. Toluene is partially ordered and occupies 40% of the volume of the crystal in the first case. Specifically each trimeric unit is separated by a molecule of toluene, which in both faces interacts through π - π interactions equal to 3.830 Å with the ring of the tetraazanaphthacene molecule of each complex. On the other hand disordered solvent toluene molecules were found in crystals of trimeric complex **16**•**TANP**•**16**.

Solid phase self-sorting properties. With the goal of examining the self-sorting of two different boronic acids when co-crystallized with an equal molar ratio of an acceptor, a solution of **TANP**, 4-chloro and 4-

bromophenylboronic acids (**10** and **11**) was placed to crystallize. As one can observe from the optical microscopy images, crystals with similar appearance were obtained (Figure 17). X-ray diffraction analysis revealed that the crystal lattice contains 40 and 60% of boronic acids **11** and **10**, respectively. Due to the similarity in the electron density between the Cl and the Br atoms, we could not unequivocally establish if each trimeric unit contains both boronic acids or only one. In terms of H-bonding distances, similar $N_1 \cdots O_2$ distances as those described in Figure 16 were measured.



Figure 17. Optical microscopy images of the single crystals obtained from the trimeric complex between **TANP** and (a) 4-chlorophenylboronic acid **10**, (b) 4-bromophenylboronic acid **11** and (c) when an equal molar solution of 4-chloro and 4-bromophenylboronic acid was used.

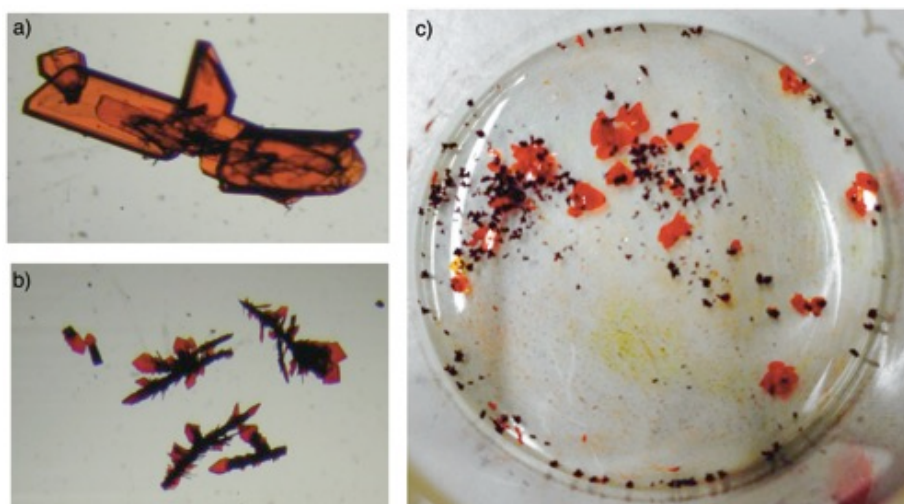


Figure 18. Optical microscopy images of the single crystals obtained from a trimeric complex between **TANP** and (a) 4-bromophenylboronic acid **11**, (b) naphthalene-1-boronic acid **16**, and (c) when an equal molar solution of both 4-bromophenyl and naphthalene-1-boronic acid was used.

However, when the same co-crystallization experiments were repeated replacing one of the two halogenated analogues with naphthalene-1-boronic acid **16**, different crystals were obtained (Figure 18c). Comparing these crystals to those obtained from separated crystallization experiments (see crystals in Figures 18a-b), one can easily conclude that the forming trimeric **X•TANP•X** complexes undergo self-sorting, leading to two types of crystals, each containing a unique 2:1 complex: **16•TANP•16** and **11•TANP•11** (Figure 18c). Single-crystal X-ray diffraction analysis of the obtained crystal mixture, revealed that crystals containing both boronic acids have never been detected in any of the analyzed samples. This means that supramolecular complexes **16•TANP•16** and **11•TANP•11** are formed and spontaneously self-sorted into two crystalline phases.

Polymeric complexes (AA•DD)_n: toward supramolecular materials. The ultimate extension to our studies was the engineering of an expanded version of these di- or trimeric non-covalent complexes systems and hence the formation of a supramolecular network. As a result, the goal was to achieve the formation of crystals containing both ditopic molecular modules **17** and **TANP**. The major experimental difficulty arising was either the poor solubility of the boronic acid in non-polar solvents or that of the acceptor in polar solvents. However, through a screening of a large variety of solvents and temperatures, we noticed that both molecules are soluble in water under reflux conditions that, by cooling down to different temperatures for a period of 24 h, gave rise to different types of crystals. For instance, when the solution is cooled at 25 °C an orange powdery precipitate was noted (Figure 19a),

whereas at 35 °C only needle-like deep red crystals of **TANP** (confirmed by X-ray analysis) were obtained (Figure 19c). However, at a cooling temperature of 30 °C the solid phase could be amended to orange flaky crystals (Figure 19b), suggesting the presence of both molecules in each crystal. This was further confirmed by single crystal X-ray diffraction analysis, revealing the formation of polymeric-like ribbons ($17 \cdot \text{TANP}$)_n, in which the single molecular components are held together by double DD•AA H-bonds. Within the polymeric assembly, N₁...O₁ and N₂...O₂ distances are equal to 2.863 Å and 2.876 Å with the boronic acid functionality being coplanar with the **TANP** aromatic structure (Figure 20a). The H-bonded ribbons supramolecularly arrange in striped patterned sheets (Figure 2b) that are organized in a multilayered, graphite-like, fashion displaying an averaged interplanar distance of 3.366 Å (Figures 20c). At the molecular level, the sheets arrange in multilayers through π - π stacking interactions, where each boronic acid aryl ring is π -sandwiched between two acceptor **TANP** molecules belonging to the nearest supramolecular sheets. As observed by optical and SEM microscopic analysis (Figures 19b and 19d-f), the sheet-like arrangement at the molecular level is expressed at higher scales, forming crystals with flaky morphologies.

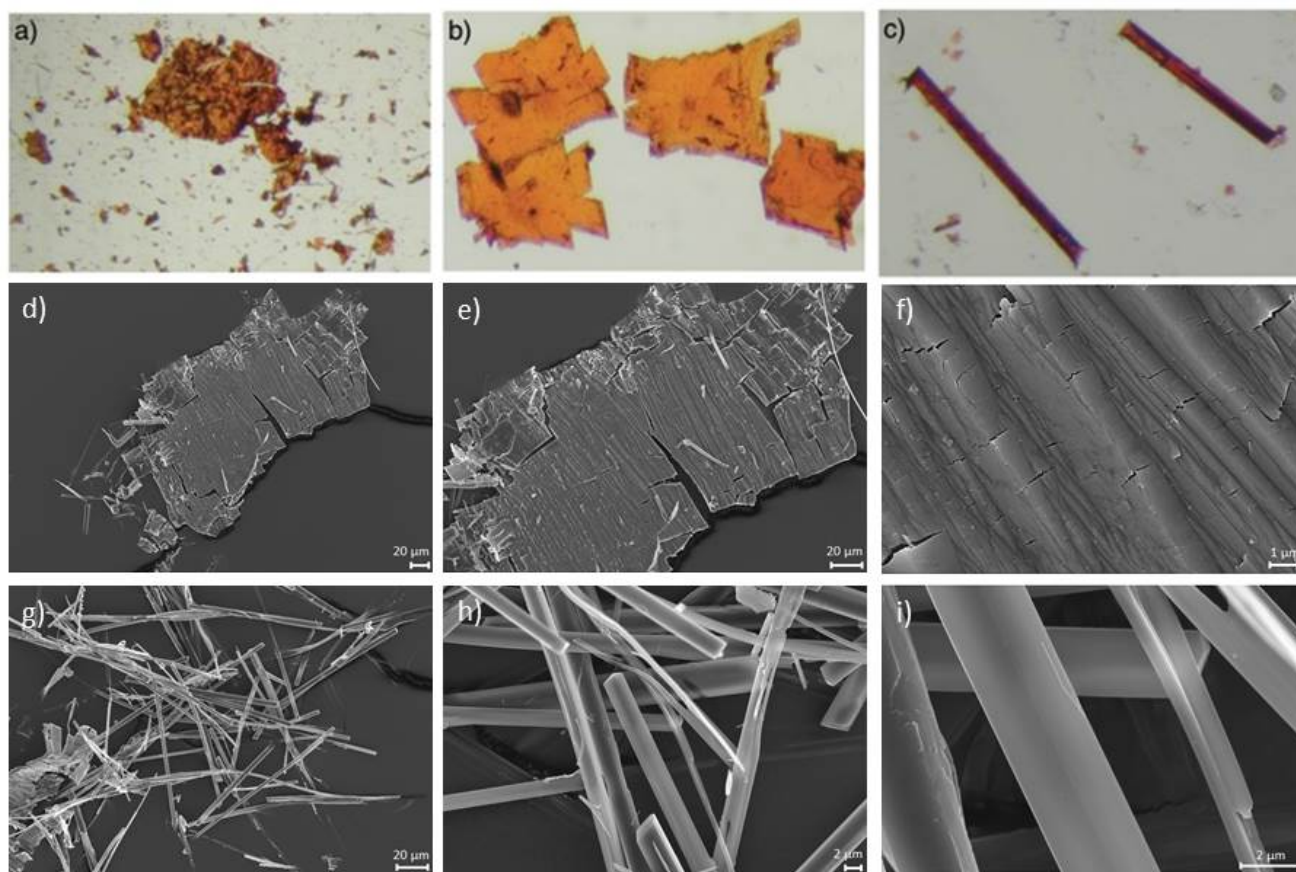


Figure 19. Optical microscopy images of the crystals obtained when an equal molar solution of 1,4-phenylenediboronic acid **17** and **TANP** were heated at 100 °C and then cooled down at (a) 25 °C, (b) 30 °C and (c) 35 °C. SEM images of a single crystal of the heteromolecular supramolecular polymer displaying an anisotropic lamellar-type organization at different magnifications: (d) 517X, (e) 1000X and (f) 20000X. SEM images of single crystals of **TANP** obtained with a cooling at 35 °C at different magnification: (g) 1000X, (h) 5000X and (i) 20000X.

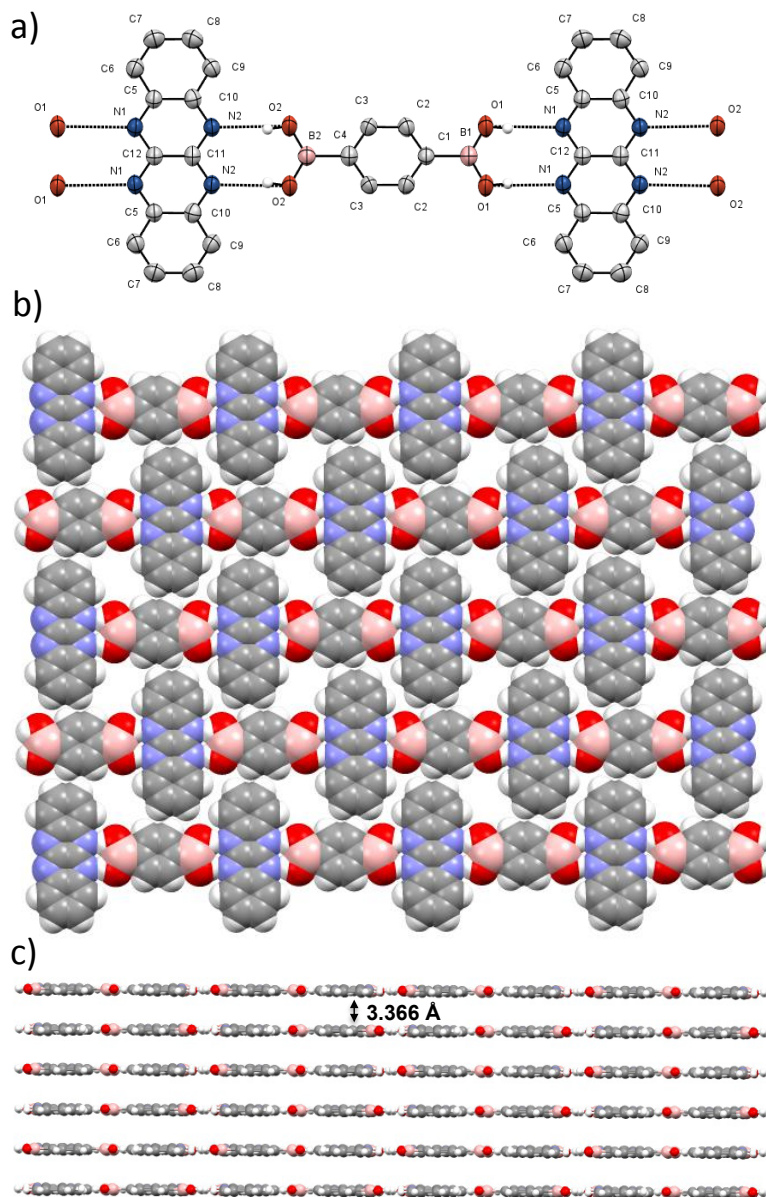


Figure 20. Crystal structure of the heteromolecular supramolecular polymer $(17\cdot\text{TANP})_n$; (a) ORTEP (drawn at the 30% probability level) representation of the crystal structure; (b) spacefill representation of in-plane zipped organization of the supramolecular polymer; (c) lamellar-like arrangement displaying interplanar distance of 3.36 Å (calculated between two planes averaging 600 atoms). Heteroatoms distances of the H-bonds: $\text{N}_1\cdots\text{O}_1$: 2.863(3) Å, $\text{N}_2\cdots\text{O}_2$: 2.876(3) Å; dihedral angle between the aryl and the boronic acid group: (a) $\text{O}_2\text{-B}_1\text{-C}_4\text{-C}_3$: $3.27(15)^\circ$, $\text{O}_1\text{-B}_1\text{-C}_1\text{-C}_2$: $1.83(15)^\circ$; space group: P2/c.

CONCLUSIONS

In summary, we have demonstrated the feasibility of aryl boronic acids to form H-bonded DD•AA type complexes with suitable acceptor partners. Most importantly determination of the K_a through solution-state binding studies of such complexes were for the first time reported. In particular, K_a ranging between 369 and 6900 M^{-1} were noted for *ortho*-substituted boronic acids analogues; values highly dependent on the substituents and on the complexation partner. **Phen** provided stronger complexes than **NAP**, possibly caused by stronger secondary electrostatic $\text{N}\cdots\text{H}$ interactions as seen by analysis of the electronic surface potential. Additional parameters taken under consideration were the K_d (homodimer formation constant) which proved to be negligible, the K_{borox} (boroxine formation constant) mainly observed when non-ortho substituted analogues are used and the K_i (hydroxyboronate ion formation) were direct evidence of its effect could not be observed. Binding studies on the solid state lead to

the formation of both dimeric 1:1, and trimeric 1:2 and 2:1 complexes. Extensive analysis of these crystal structures revealed that “flat” complexes are the result of non-*ortho* substituted boronic acids in contrast with “T-shaped” complexes arising from more sterically demanding *ortho* substituted analogues. Hence, showcasing their unique ability to self-adapt retaining their recognition property. The existence of π - π interactions in both the dimeric and trimeric complexes is affected by the presence and bulkiness of the *ortho* substituents, a parameter that influences the distance of the H-bond as well. The results obtained in solution are in accordance with the solid state since shorter H-bond distances are noted in the cases where **Phen** is the complexation partner. To the best of our knowledge this paper for the first time describes a supramolecular H-bonded polymer involving a boronic acid, successfully constructed through host-guest interaction between ditopic 1,4-phenyldiboronic acid and **TANP**. The highly ordered mono dimensional polymeric material produced features infinite ribbon-like arrays running parallel as observed through SEM analysis. We believe this study further strengthens the potential of the boronic acid functional group as a building blocks potent in supramolecular chemistry, not only as dynamic reactive species for dynamic covalent chemistries, but also through H-bond recognition. Future challenges would be to apply this principle in the considerate choice of complexation partners resulting in the construction of functional and operative supramolecular architectures both in the solid state and in solution, which could feature structural and physical properties useful in areas such as organic materials for printed electronics and organocatalysis.

ASSOCIATED CONTENT

Synthetic protocols, spectroscopic characterizations, titration experiments, theoretical details and X-ray parameters. This material is available free of charge via the Internet at <http://pubs.acs.org>

AUTHOR INFORMATION

Corresponding Author

*bonifazid@cardiff.ac.uk

ACKNOWLEDGMENT

D.B. gratefully acknowledges the EU through the ERC Starting Grant “COLORLANDS”, the Wallon Region for the ‘Flycoat’ projects, the Science Policy Office of the Belgian Federal Government (BELSPO-IAP 7/05 project). A.R. thanks the FRS-FNRS for his FRIA fellowship. Ms. Florence Valtin is acknowledged for her help in the preparation of the first boronic acids in the frame of her master thesis. Prof. Paolo Tecilla (University of Trieste) is also acknowledged for the discussion and help with the fitting of the dimerization equilibrium of boronic acids and the discussion about the 1:1 binding model of the heteromolecular H-bonded complexes. The authors thank the physical chemistry and characterization (PC²) at the UNamur and Bernadette Norberg for the X-ray measurements and data interpretation.

REFERENCES

- (1) Hall, D. *Boronic Acids: Preparation and Applications in Organic Synthesis and Medicine*; Wiley-VCH: Weinheim, 2005.
- (2) (a) James, T. D. *Beilstein J. Org. Chem.* **2016**, *12*, 391. (b) Nishiyabu, R.; Kubo, Y.; James, T. D.; Fossey, J. S. *Chem. Commun.* **2011**, *47*, 1124. (c) Kubo, Y.; Nishiyabu, R.; James, T. D. *Chem. Commun.* **2015**, *51*, 2005; (d) Fujita, N.; Shinkai, S.; James, T. D. *Chem. Asian J.* **2008**, *3*, 1076. (e) Corbett, P. T.; Leclaire, J.; Vial, L.; West, K. R.; Wietor, J. L.; Sanders, J. K. M.; Otto, S. *Chem. Rev.* **2006**, *106*, 3652.
- (3) For some topical see: (a) Nishiyabu, R.; Kubo, Y.; James, T. D.; Fossey, J. S. *Chem. Commun.* **2011**, *47*, 1106. (b) Brooks, W. L. A.; Sumerlin, B. S. *Chem. Rev.* **2016**, *116*, 1375. (c) Sun, X.; James T. D. *Chem. Rev.* **2015**, *115*, 8001. (d) Wu, J.; Kwon, B.; Liu, W.; Anslyn, E. V.; Wang, P.; Kim, J. S. *Chem. Rev.* **2015**, *115*, 7893. (e) You, L.; Zha, D.; Anslyn, E. V. *Chem. Rev.* **2015**, *115*, 7840. (f) Li, M.; Zhu, W., Marken, F.; James, T. D. *Chem. Commun.*, **2015**, *51*, 14562. Selected recent papers in the field: (f) Oesch, D.; Luedtke; N. W. *Chem. Commun.* **2015**, *51*, 12641. (g) Zhong, Z.; Anslyn, E. V. *J. Am. Chem. Soc.*, **2002**, *124*, 9014. (h) Zhu, L.; Anslyn, E. V. *J. Am. Chem. Soc.*, **2004**, *126*, 3676. (i) Zhu, L.; Zhong, Z.; Anslyn, E. V. *J. Am. Chem. Soc.*, **2005**, *127*, 4260. Su, X.; Zhai, W.; Fossey, J. S.; James, T. D. *Chem.*

- Commun.*, **2016**, *52*, 3456. Su, X.; Xu, S.-Y.; Flower, S. E.; Fossey, Qian, X.; J. S.; James, T. D. *Chem. Commun.*, **2013**, *49*, 8311.
- (4) (a) Aelvoet, K.; Batsanov, A. S.; Blatch, A. J.; Grosjean, C.; Patrick, L. G. F.; Smethurst, C. A.; Whiting, A. *Angew. Chem. Int. Ed.* **2008**, *47*, 768. (b) Ilyashenko, G.; Georgiou I.; Whiting, A. *Acc. Chem. Res.* **2009**, *42*, 756.
- (5) For some topical reviews see: (a) Rowan, S. J.; Cantrill, S. J.; Cousins, G. R. L.; Sanders, J. K. M.; Stoddart, J. F. *Angew. Chem. Int. Ed.* **2002**, *41*, 898. (b) Lehn, J.M. *Chem. Soc. Rev.*, **2007**, *36*, 151. (c) Jin, Y.; Yu, C.; Denman, R. J.; Zhang, W. *Chem. Soc. Rev.* **2013**, *42*, 6634. (d) Wilson, A.; Gasparini, G.; Matile, S. *Chem. Soc. Rev.* **2014**, *43*, 194. Selected recent papers in the field: (e) Rodriguez-Docampo, Z.; Otto, S. *Chem. Commun.* **2008**, 5301; (f) Sarma, R. J.; Otto, S.; Nitschke, J. R. *Chem. Eur. J.* **2007**, *13*, 9542. (g) Lascano, S.; Zhang, K.-D.; Wehlauch, R.; Gademann, K.; Sakai, N.; Matile, S. *Chem. Sci.* **2016**, *7*, 4720. (h) Zhang, K.-D.; Sakai, N.; Matile, S. *Org. Biomol. Chem.* **2015**, *13*, 8687. (i) Zhang, K.-D.; Matile, S. *Angew. Chem. Int. Ed.* **2015**, *54*, 8980. (j) Fin, A.; Petkova, I.; Alonso Doval, D.; Sakai, N.; Vauthey, E.; Matile, S. *Org. Biomol. Chem.*, **2011**, *9*, 8246. (k) Rocard, L.; Berenzin, A.; De Leo, F.; Bonifazi, D. *Angew. Chem. Int. Ed.* **2015**, *54*, 15739. (l) Nishiyabu, R.; Tereoka, S.; Matsushima, Y.; Kubo, Y. *Angew. Chem. Int. Ed.* **2012**, *77*, 201. (m) Seifert, H. M.; Trejo, K. R.; Anslyn, E. V. *J. Am. Chem. Soc.* **2016**, *138*, 10916. (n) Christinat, N.; Croisier, E.; Scopelliti, R.; Cascella, M.; Roethlisgerger, U.; Severin, K. *Eur. J. Inorg. Chem.* **2007**, 5177. (o) Colson, J. W.; Woll, A. R.; Mukherjee, A.; Levendorf, M. P.; Spitler, E. L.; Shields, V. B.; Spencer, M. G.; Park, J.; Dichtel, W. R. *Science* **2011**, *332*, 228.
- (6) (a) Iwasawa, N.; Takahagi, H. *J. Am. Chem. Soc.* **2007**, *129*, 7754. (b) Kataoka, K.; Okuyama, S.; Minami, T.; James, T. D.; Kubo, Y. *Chem. Commun.* **2009**, 1682. (c) Kataoka, K.; James, T. D.; Kubo, Y. *J. Am. Chem. Soc.* **2007**, *129*, 15126. (d) Takahagi, H.; Fujibe, S.; Iwasawa, N. *Chem. Eur. J.* **2009**, *15*, 13327. (e) Li, Y.; Ding, J.; Day, M.; Tao, Y.; Lu, J.; D'Iorio, M. *Chem. Mater.* **2003**, *15*, 4936.
- (7) (a) Iovine, P. M.; Gyselbrecht, C. R.; Perttu, E. K.; Klick, C.; Neuwelt, A.; Loera, J.; Di Pasquale, A. G.; Rheingold, A. L.; Kua, J. *Dalton Trans.* **2008**, 3791. (b) Perttu, E. K.; Arnold, M.; Iovine, P. M. *Tetrahedron Lett.* **2005**, *46*, 8753. (c) Côté, A. P.; Benin, A. I.; Ockwig, N. W.; O'Keeffe, M.; Matzger, A. J.; Yaghi, O. M. *Science* **2005**, *310*, 1166.
- (8) (a) Kameta, N.; Hiratani, K. *Tetrahedron Lett.* **2006**, *47*, 4947. (b) Kameta, N.; Hiratani, K. *Chem. Commun.* **2005**, 725. (c) Danjo, H.; Hirata, K.; Yoshigai, S.; Azumaya, I.; Yamaguchi, K. *J. Am. Chem. Soc.* **2009**, *131*, 1638.
- (9) Campos-Gaxiola, J. J.; Vega-Paz, A.; Román-Bravo, P.; Höpfl, H.; Sánchez-Vázquez, M. *Cryst. Growth Des.* **2010**, *10*, 3182.
- (10) (a) Rettig, S. J.; Trotter, J. *Can. J. Chem.* **1977**, *55*, 3071. (b) Allen, F. H. *Acta Cryst.* **2002**, *B58*, 380. (c) Cyrański, M. K.; Jezierska, A.; Klimentowska, P.; Panek, J. J.; Sporzyński, A. *J. Phys. Org. Chem.* **2008**, *21*, 472.
- (11) (a) Fournier, J. H.; Maris, T.; Wuest, J. D.; Guo, W.; Galoppini, E. *J. Am. Chem. Soc.* **2003**, *125*, 1002. (b) Wuest, J. D. *Chem. Commun.* **2005**, 5830. (c) Maly, K. E.; Malek, N.; Fournier, J. H.; Rodríguez-Cuamatzi, P.; Maris, T.; Wuest, J. D. *Pure Appl. Chem.* **2006**, *78*, 1305..
- (12) (a) Adamczyk-Woźniak, A.; Cyrański, M. K.; Dąbrowska, A.; Gierczyk, B.; Klimentowska, P.; Schroeder, G.; Zubrowska, A.; Sporzyński, A. *J. Mol. Struct.* **2009**, *920*, 430. (b) Cyrański, M. K.; Klimentowska, P.; Rydzewska, A.; Serwatowski, J.; Sporzyński, A.; Stępień, D. K. *Cryst. Eng. Comm.* **2012**, *14*, 6282. (c) Adamczyk-Woźniak, A.; Brzózka, Z.; Dąbrowski, M.; Madura, I. D.; Scheidsbach, R.; Tomecka, E.; Żukowski, K.; Sporzyński, A. *J. Mol. Struct.* **2013**, *1035*, 190.
- (13) (a) Scouten, W. H.; Liu, X. C.; Khangin, N.; Mullica, D. F.; Sappenfield, E. L. *J. Chem. Crystallogr.* **1994**, *24*, 621. (b) Zhao, J.; Davidson, M. G.; Mahon, M. F.; Kociok-Köhn, G.; James, T. D. *J. Am. Chem. Soc.* **2004**, *126*, 16179. (c) Coghlan, S. W.; Giles, R. L.; Howard, J. A. K.; Patrick, L. G. F.; Probert, M. R.; Smith, G. E.; Whiting, A. *J. Organomet. Chem.* **2005**, *690*, 4784. (d) Yoshino, J.; Kano, N.; Kawashima, T. *Tetrahedron* **2008**, *64*, 7774. (e) Adamczyk-Woźniak, A.; Brzózka, Z.; Cyrański, M. K.; Filipowicz-Szymańska, A.; Klimentowska, P.; Żubrowska, A.; Żukowski, K.; Sporzyński, A. *Appl. Organometal. Chem.* **2008**, *22*, 427. (f) Adamczyk-Woźniak, A.; Madura, I.; Pawełko, A.; Sporzyński, A.; Żubrowska, A.; Żyta, J. *Cent. Eur. J. Chem.* **2011**, *9*, 199. (g) Adamczyk-Woźniak, A.; Fratila, R. M.; Madura, I. D.; Pawełko, A.; Sporzyński, A.; Tumanowicz, M.; Velders, A. H.; Żyta, J. *Tetrahedron Lett.*

- 2011**, 52, 6639. (h) Adamczyk-Woźniak, A.; Cyrański, M. K.; Frączak, B. T.; Lewandowska, A.; Madura, I. D.; Sporzyński, A. *Tetrahedron* **2012**, 68, 3761.
- (14) (a) Luliński, S.; Madura, I.; Serwatowski, J.; Szatyłowicz, H.; Zachara, J. *New J. Chem.* **2007**, 31, 144. (b) Rodríguez-Cuamatzi, P.; Tlahuext, H.; Höpfl, H. *Acta Cryst.* **2009**, E65, o44. (c) Durka, K.; Gontarczyk, K.; Kliś, T.; Serwatowski, J.; Woźniak, K. *Appl. Organometal. Chem.* **2012**, 26, 287. (d) Durka, K.; Jarzemska, K. N.; Kamiński, R.; Luliński, S.; Serwatowski, J.; Woźniak, K. *Cryst. Growth Des.* **2012**, 12, 3720; (e) Madura, I. D.; Czerwińska, K.; Soldańska, D. *Cryst. Growth Des.* **2014**, 14, 5912.
- (15) Sakakura, A.; Yamashita, R.; Ohkubo, T.; Akakura, M.; Ishihara, K. *Aust. J. Chem.* **2011**, 64, 1458.
- (16) (a) Regueiro-Figueroa, M.; Djanashvili, K.; Esteban-Gómez, D.; de Blas, A.; Platas-Iglesias, C.; Rodríguez-Blas, T. *Eur. J. Org. Chem.* **2010**, 3237. (b) SeethaLekshmi, N.; Pedireddi, V. R. *Cryst. Growth Des.* **2007**, 7, 944.
- (17) (a) Rodríguez-Cuamatzi, P.; Arillo-Flores, O. I.; Bernal-Uruchurtu, M. I.; Höpfl, H. *Cryst. Growth Des.* **2005**, 5, 167. (b) Rogowska, P.; Cyrański, M. K.; Sporzyński, A.; Ciesielski, A. *Tetrahedron Lett.* **2006**, 47, 1389. (c) Aakeröy, C. B.; Desper, J.; Levin, B. *Cryst. Eng. Comm.* **2005**, 7, 102. (d) Pedireddi, V. R.; SeethaLekshmi, N. *Tetrahedron Lett.* **2004**, 45, 1903. (e) Rodríguez-Cuamatzi, P.; Luna-García, R.; Torres-Huerta, A.; Bernal-Uruchurtu, M. I.; Barba, V.; Höpfl, H. *Cryst. Growth Des.* **2009**, 9, 1575. (f) Talwelkar, M.; Pedireddi, V. R. *Tetrahedron Lett.* **2010**, 51, 6901. (g) Varughese, S.; Azim, Y.; Desiraju, G. R. *J. Pharm. Sci.* **2010**, 99, 3743. (h) Varughese, S.; Sinha, S. B.; Desiraju, G. R. *Sci. China Chem.* **2011**, 54, 1909.
- (18) Wang, J. and Zhang, Y. *ACS Cat.* **2016**, 6, 4871.
- (19) (a) Echavarren, A.; Galan, A.; Lehn, J. M.; de Mendoza, J. *J. Am. Chem. Soc.* **1989**, 111, 4994. (b) Segura, M.; Alcazar, V.; Prados, P.; de Mendoza, J. *Tetrahedron* **1997**, 53, 13119.
- (20) (a) Jorgensen, W. L.; Pranata, J. *J. Am. Chem. Soc.* **1990**, 112, 2008. (b) Kawahara, S.; Uchimar, T. *J. Comput. Chem. Jpn.* **2004**, 3, 41. (c) Djurdjevic, S.; Leigh, D. A.; McNab, H.; Parsons, S.; Teobaldi, G.; Zerbetto, F. *J. Am. Chem. Soc.* **2007**, 129, 476.
- (21) (a) Isoda, K.; Nakamura, M.; Tatenuma, T.; Ogata, H.; Sugaya, T.; Tadokora, M. *Chem. Lett.* **2012**, 41, 937. (b) Rashkin, M. J.; Hughes, R. M.; Calloway, N. T.; Waters, M. L. *J. Am. Chem. Soc.* **2014**, 126, 13320.
- (22) (a) Sijbesma, R. P., *Science* **1997**, 278, 1601-1604; (b) Brunsveld, L.; Folmer, B. J. B.; Meijer, E. W.; Sijbesma, R. P., *Chem. Rev.* **2001**, 101, 4071-4098; (b) de Greef, T. F. A.; Meijer, E. W. *Nature*, **2008**, 453, 171. (c) De Greef, Tom F. A.; Smulders, Maarten M. J.; Wolffs, Martin; Schenning, Albert P. H. J.; Sijbesma, Rint P.; Meijer, E. W. *Chem. Rev.*, **2009**, 109, 5687. (d) Aida, T.; Meijer, E. W.; Stupp, S. I. *Science*, **2012**, 335, 813.
- (23) Larkin, J. D.; Bhat, K. L.; Markham, G. D.; Brooks, B. R.; Schaefer III, H. F.; Bock, C. W. *J. Phys. Chem. A* **2006**, 110, 10633.
- (24) (a) Tokunaga, Y.; Ueno, H.; Shimomura, Y. *Heterocycles* **2007**, 74, 219. (b) Tokunaga, Y.; Ueno, H.; Shimomura, Y.; Seo, T. *Heterocycles* **2002**, 57, 787. (c) Spitler, E. L.; Giovino, M. R.; White, S. L.; Dichtel, W. R. *Chem. Sci.* **2011**, 2, 1588.
- (25) (a) Beijer, F. H.; Sijbesma, R. P.; Vekemans, J. A. J. M.; Meijer, E. W.; Kooijman, H.; Spek, A. L. *J. Org. Chem.* **1996**, 61, 6371. (b) Đorđević, L.; Marangoni, T.; Miletić, T.; Rubio-Magnieto, J.; Mohanraj, J.; Amenitsch, H.; Pasini, D.; Liaros, N.; Couris R, S.; Armaroli, N.; Surin, M.; Bonifazi, D. *J. Am. Chem. Soc.* **2015**, 137, 8150. (c) Goldberg, A. R.; Northrop, B. H. *J. Org. Chem.* **2016**, 81, 969.
- (26) (a) Lorand, J. P.; Edwards, J. O. *J. Org. Chem.* **1959**, 24, 769. (b) Pizer, R.; Tihal, C. *Inorg. Chem.* **1992**, 31, 3243. (c) Watanabe, E.; Miyamoto, C.; Tanaka, A.; Iizuka, K.; Iwatsuki, S.; Inamo, M.; Takagi, H. D.; Ishihara, K. *Dalton Trans.* **2013**, 42, 8446. (d) Okamoto, T.; Tanaka, A.; Watanabe, E.; Miyazaki, T.; Sugaya, T.; Iwatsuki, S.; Inamo, M.; Takagi, H. D.; Odani, A.; Ishihara, K. *Eur. J. Inorg. Chem.* **2014**, 2389. (e) Furikado, Y.; Nagahata, T.; Okamoto, T.; Sugaya, T.; Iwatsuki, S.; Inamo, M.; Takagi, H. D.; Odani, A.; Ishihara, K. *Chem. Eur. J.* **2014**, 20, 13194.
- (27) (a) Tomsho, J. W.; Benkovic, S. J. *J. Org. Chem.* **2012**, 77, 2098. (b) Ni, W.; Fang, H.; Springsteen, G.; Wang, B. *J. Org. Chem.* **2004**, 69, 1999. (c) Fan, X.; Freslon, S.; Daguebonne, C.; Pollès, L. L.; Calvez, G.; Bernot, K.; Yi, X.; Huang, G.; Guillou, O. *Inorg. Chem.* **2015**, 54, 5534.
- (28) Thordarson, P. *Chem. Soc. Rev.* **2011**, 40, 1305.

- (29) (a) Zimmerman, S. C.; Murray, T. J. *Tetrahedron Lett.* **1994**, *35*, 4077. (b) Sartorius, J.; Schneider, H. J. *Chem. Eur. J.* **1996**, *2*, 1446. (c) Tamashiro, B. T.; Cedano, M. R.; Pham, A. T.; Smith, D. K. *J. Phys. Chem. C* **2015**, *119*, 12865.
- (30) Cook, J. L.; Hunter, C. A.; Low, C. M. R.; Perez-Velasco, A.; Vinter, J. G. *Angew. Chem. Int. Ed.*, **2007**, *46*, 3706.
- (31) (a) Mukherjee, A.; Tothadi, S.; Desiraju, G. R. *Acc. Chem. Res.* **2014**, *47*, 2514. (b) Tothadi, S.; Joseph, S.; Desiraju, G. R. *Cryst. Growth. Des.* **2013**, *13*, 3242. (c) Bui, T. T. T.; Dahaoui, S.; Lecomte, C.; Desiraju, G. R.; Espinosa, E. *Angew. Chem. Int. Ed.* **2009**, *48*, 3838.
- (32) Isoda, K.; Nakamura, M.; Tatenuma, T.; Ogata, H.; Sugaya, T.; Tadokoro, M. *Chem. Lett.* **2012**, *41*, 937.

For Table of Contents Only

